AD-A157 669 IMPROVED TECHNIQUES FOR THE GROWTH OF HIGH QUALITY CADMIUM TELLURIDE CRYS. (U) STANFORD UNIV CA CENTER FOR MATERIALS RESEARCH R S FEIGELSON ET AL. JUN 85 1/1

UNCLASSIFIED CMR-85-3 ARO-19489.3-EL DAAG29-83-K-0023 F/G 20/2 NL

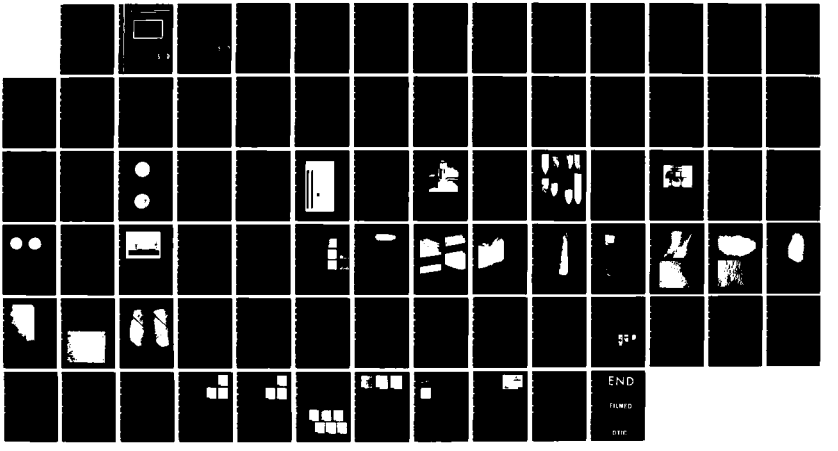

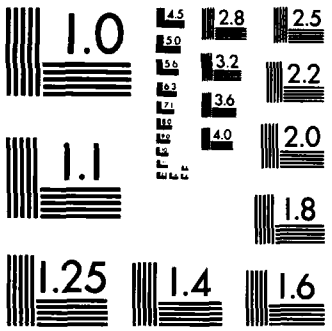

MICROCOPY RESOLUTION TEST CHART
NATIONAL BUREAU OF STANDARDS-1963-A

(2)

Final Report

on

IMPROVED TECHNIQUES FOR THE GROWTH OF HIGH QUALITY CADMIUM TELLURIDE CRYSTALS

Submitted to
U. S. Army Research Office
Research Triangle Park, NC 27709
Contract No. DAAG29-83-K-0023

CMR-85-3
June, 1985

CENTER FOR MATERIALS RESEARCH

STANFORD UNIVERSITY • STANFORD, CALIFORNIA

Center for Materials Research
McCullough Building
Stanford University
Stanford, CA 94305

Final Report

on

IMPROVED TECHNIQUES FOR THE GROWTH OF HIGH QUALITY CADMIUM TELLURIDE CRYSTALS

Submitted to
U. S. Army Research Office
Research Triangle Park, NC 27709
Contract No. DAAG29-83-K-0023

CMR-85-3
June, 1985

Submitted by
The Board of Trustees of
The Leland Stanford Jr. University
Stanford, California 94305

Principal Investigator:

Professor Robert S. Feigelson
Center for Materials Research

Associate Investigator

Dr. Roger K. Route
Center for Materials Research

UNCLASSIFIED

SECURITY CLASSIFICATION OF THIS PAGE (When Data Entered)

REPORT DOCUMENTATION PAGE	READ INSTRUCTIONS BEFORE COMPLETING FORM
1. REPORT NUMBER: ARO 19489.3-EL	2. GOVT ACCESSION NO. AD-A157669 — 3. RECIPIENT'S CATALOG NUMBER
4. TITLE (and Subtitle): Improved Techniques for the Growth of High Quality Cadmium Telluride Crystals	5. TYPE OF REPORT & PERIOD COVERED: Final Technical Report 1/1/82 - 12/31/84
	6. PERFORMING ORG. REPORT NUMBER: CMR-85-3
7. AUTHOR(s): R. S. Feigelson, R. K. Route	8. CONTRACT OR GRANT NUMBER(s): DAAG29-83-K-0023
9. PERFORMING ORGANIZATION NAME AND ADDRESS: Center for Materials Research, Stanford University, Stanford, CA 94305	10. PROGRAM ELEMENT, PROJECT, TASK AREA & WORK UNIT NUMBERS
11. CONTROLLING OFFICE NAME AND ADDRESS: U. S. Army Research Office, Post Office Box 12211, Research Triangle Park, NC 27709	12. REPORT DATE: June 1985
	13. NUMBER OF PAGES
14. MONITORING AGENCY NAME & ADDRESS(if different from Controlling Office)	15. SECURITY CLASS. (of this report): Unclassified
	15a. DECLASSIFICATION/DOWNGRADING SCHEDULE

16. DISTRIBUTION STATEMENT (of this Report)

Approved for public release; distribution unlimited.

17. DISTRIBUTION STATEMENT (of the abstract entered in Block 20, if different from Report)

NA

18. SUPPLEMENTARY NOTES

The view, opinions, and/or findings contained in this report are those of the author(s) and should not be construed as an official Department of the Army position, policy, or decision, unless so designated by other documentation.

19. KEY WORDS (Continue on reverse side if necessary and identify by block number)

CdTe, Cadmium Telluride, Crystal Growth, Growth Interface Shapes in, Etching Studies in, X-ray Topography, Defects in,

20. ABSTRACT (Continue on reverse side if necessary and identify by block number)

This report summarizes two years' work as part of a multiyear program on improved techniques for the growth of high quality cadmium telluride crystals and represents one of the most comprehensive studies of melt growth and defect characterization in CdTe reported to date. Extensive melt growth studies were carried out using the vertical Bridgman method. Growth parameters were systematically varied in order to determine the influence of seed orientation, thermal environment, and growth rate on crystal quality. Growth interface shapes were revealed using (cont)

DD FORM 1 JAN 73 1473 EDITION OF 1 NOV 65 IS OBSOLETE

UNCLASSIFIED

SECURITY CLASSIFICATION OF THIS PAGE (When Data Entered)

Block 20 continued

autoradiographic dopant tracing methods. Melt thermal profiling was also carried out to further evaluate growth interface shapes. Controlled convex growth interface shapes were generated by using the heat exchanger method. By this means some improvement in grain structure of the typically polycrystalline boules was accomplished. Low frequency melt vibrations during growth were also observed to improve grain structure and reduce dislocation density.

Extensive defect characterization was also carried out using chemical etching methods, and later, synchrotron x-ray topography. Comparative studies of a broad selection of commercial CdTe substrates was carried out, and extensive defect structure was observed in all cases. Reduced dislocation densities and defect structures were accomplished using both low amplitude melt vibrations and doping with $In^{III}Cl_3$. In the second case, solution hardening was assumed to be the mechanism responsible. For the case of melt vibration, the mechanism is not yet understood.

TABLE OF CONTENTS

TABLES, ILLUSTRATIONS AND APPENDICES

IMPROVED TECHNIQUES FOR THE GROWTH OF HIGH QUALITY CADMIUM TELLURIDE CRYSTALS

A Final Report

I. Introduction

This final report summarizes two years' work as part of a multi-year program on "Improved Techniques for the Growth of Cadmium Telluride Crystals." A preliminary program of one year's duration with support from ANVEOL, Contract No. DAAK-70-81-K-0262, was used to initiate the research effort. Continuing funding at a somewhat higher level was then obtained from ARO to support an in-depth research effort. The overall research plan described herein was based on a program of three-years' duration although the initial funding was for only a two-year period.

Follow-on funding was not received at the end of the two-year period and the research then in progress was concluded using partial support from NSF through the NSF/MRL program at Stanford Universty. At the time of its conclusion, the program was already highly successful. New scientific knowledge had been gained, two refereed papers had been published, and two important areas for further research had been identified. Cadmium telluride is still an important material for a number of technologial applications, and research in this particular area, improving its growth technology and defect characterization, should be continued.

A. Program Objectives

This research program was intended to study in a systematic and precise manner the growth of high quality CdTe crystals. The effects of low frequency mechanical vibrations, thermal environment, and oriented growth were to be studied during Bridgman-Stockbarger growth of CdTe crystals. Crystal growth experiments from suitably doped or undoped stoichiometric melts and Te-rich solutions were to be carried out in thoroughly instrumented growth systems to ascertain the effects of the above factors on the grain structure, boule singularity, compositional and electrical uniformity, and crystalline defect distribution. Thorough evaluation of macroscopic and microscopic growth

defects were to be carried out using a variety of analytical methods. The ultimate objective of the program was the development of techniques to improve the quality of CdTe boules with respect to singularity and compositional uniformity, and to improve reproducibility, yield rates, and crystal size.

B. Background

The motivation for this program was the widespread inability to reproducibly grow large, high quality single crystal boules of CdTe both in industrial and research laboratory settings. A considerable amount of effort has been devoted to bulk crystal growth techniques with this goal in mind, including melt growth by the Bridgman method, zone refining, travelling solvent method, travelling heater method, solution growth from both Cd-rich and Te-rich solutions, and physical vapor transport. Each of these methods occasionally produce high quality single crystal boules, but the yields tend to be low and there were usually other problem areas such as slow growth rates, solvent inclusions, etc.

A second problem area with CdTe crystals is their high defect density. Etch pit densities in substrate material are often in the 10^4 - 10^6 cm^{-2} range. In this laboratory, it was discovered some years ago that the application of low amplitude, 60 Hz mechanical vibrations to a vertical Bridgman-Stockbarger system resulted in a dramatic improvement in the crystal quality of typical 18-20 mm CdTe boules. Control boules went from large grain poly to virtually single crystal in a significant fraction of cases. This phenomenon was not then understood but occurred with excellent statistical correlation. In Fig. 1 we show cross-sections from typical 18 mm CdTe boules grown with and without the application of low amplitude 60 Hz mechanical vibrations. We also found that in most cases the virtually single crystal boules displayed surprisingly lower etch pit densities by factors of 10^2 or more when compared to control boules.

Concurrently, a technique for producing precision tapered quartz growth ampoules by vacuum forming was developed. This allowed us to seed Bridgman boules of certain materials in any growth direction

desired and to virtually eliminate mechanical interactions with the quartz ampoules.

This research program grew out of these developments. Its intent was to study first the effect of growth orientation on the structure of CdTe boules and then to identify the mechanism by which improved crystallinity is achieved with the use of low amplitude mechanical vibrations and to optimize the process.

C. Approach to the Problem

An initial goal of this program was to determine an otherwise optimum set of Bridgman growth parameters so that the melt vibration variable could be studied effectively. This goal, by necessity, required that we carry out the first comprehensive and broad ranging study of growth system variables in the CdTe system. CdTe crystals 28 mm in diameter were grown by the vertical Bridgman method under a wide range of system parameters using the technology developed in the preliminary NVEOL-supported program. Growth system parameters were to be determined by thermal probing, radiographic growth interface shape studies, and in-situ thermal probing. All growth system variables were then to be correlated with the macroscopic grain structure and the microscopic defect structure.

A second goal was to advance the study of point and line defects in CdTe, by first extending the chemical etching method to gain improved reliability and additional information. This work would further ellucidate the apparent discrepancy with TEM results on dislocation densities that were carried out in our earlier program. Two chemical etching solutions were to be emphasized, those developed by Inoue [1], and those developed by Nakagawa [2]. Secondly, we planned to bring more advanced analytical technologies to bear on the study of dislocations, and how they relate back to the growth parameters in this system.

II. Program Summary

This section summarizes our most significant research results and identifies important areas for further study. The program has resulted in two publications which are reprinted in total as Appendix I and Appendix II. These will be referred to in appropriate sections of the text.

A. Optimization of Crystal Growth Parameters

To isolate the effects of mechanical vibrations in the CdTe system, we first set out to develop an otherwise optimum set of growth system variables. This was done to minimize the structural variations that inevitably occur from one boule to another in CdTe. This effort quickly evolved into a broad ranging and comprehensive study of vertical Bridgman growth system parameters.

1. Crystal Growth Equipment

Vertical Bridgman crystal growth experiments were carried out in two furnace systems having 2.5" bores and precision stepless dc motor tachometer drives. These units were developed during the NVEOL program. Through the use of end zone superheaters and adjustable slaved "Variacs," thermal profiles with a range of temperature gradients at the growth interface could be achieved (Fig. 2).

Vacuum-forming on carbon mandrels was routinely used to produce precision-tapered 28 mm ID growth ampoules of fused silica. Internal tapers were typically .75° to reduce keying and to allow the boules to slide out easily after growth. Two styles of growth ampoules were used for a majority of the growth experiments: (1) a standard Bridgman configuration with a square cross-section seed pocket to accommodate seed bars 8 mm^2 x 50 mm long, and (2) a flat-bottomed but still tapered ampoule having no seed pocket or flare-out region. See Fig. 3. All crystal growth crucibles were internally coated with an opaque layer of carbon by the pyrolysis at 1000°C of hexane carried on an argon stream.

A majority of growth experiments were carried out with the appli-

cation of low amplitude 60 Hz mechanical vibrations. The overall system schematic, including a thermocouple used to control seed attachment, is shown in Fig. 4a and a photograph of a typical vibrational test fixture in Fig. 4b.

2. Seed and Charge Materials

Oriented 8 mm^2 bars were mined out of large-grain polycrystalline boules for use as seeds. In some cases these contained twins which were useful in determining the melt-back interfaces. Charge material during the initial 15 months was synthesized in our laboratories from 5-9's Cd shot and Te polycrystalline ingot (Comineo, Inc.). We typically reacted the CdTe from slightly Te-rich (+0.1%) compositions to avoid ampoule failure. These were unidirectionally solidified in quartz ampoules and the last-to-freeze sections removed prior to being used for controlled growth experiments. During the remaining nine months, we used 1 kg CdTe ingots (nominally 5-9's) from II-VI, Inc. as feedstock. In general, the II-VI material behaved identically to our own: no metallic impurities were detectable in either, and their DTA melting curves were in fact slightly "cleaner" than our own material which we anticipated because ours contained a slight Te excess.

3. Growth Parameter Studies

Standard crystal growth conditions following earlier work were established and each system variable was then systematically varied from one run to the next. Nominal crystal growth parameters were: growth rate = 1 mm/hour, temperature gradient at growth interface = 18°C/cm in open bore = 10°C/cm with crucible in position, growth ampoule evacuated to 10^{-5} torr before sealing, and 60 Hz low amplitude vibration present. Peak vibrational amplitude in the vertical direction was measured using a single axis accelerometer and was found to be a $\simeq$ 0.005g. In all, a total of 45 separate crystal growth experiments were carried out, Table I, varying the growth parameters identified in Table II.

Initially seed orientation was thought to be the most likely major influence on CdTe cystal quality. However, no seed orientation was found to propagate without breaking down. Once having broken

III. Program Assessment and Recommendations

At the end of this 24 month research program, a number of conclusions and observations can be made. The program has been highly successful from our point of view in that it has contributed significant new knowledge on the growth of a particularly useful material. We regret that a full three-year period was not available to complete much of the work begun here. Non-the-less, two refereed publications did result and the groundwork for several more important studies has been laid.

There is not much question that low amplitude mechanical vibrations can have a positive influence in certain crystal growth situations, including the growth of CdTe. Systematic studies of this parameter were never really achieved in this work because of its early conclusion. We feel strongly that this particular growth parameter still merits a systematic, careful study.

Crystal growth using the heat exchanger method makes it possible to gain some control over the melt/solid growth interface shape, an important growth parameter in most materials systems. Preliminary experiments did verify interface shape control and seemed to indicate enhanced grain selectivity and improved grain structure. We propose this as one area where further research would be valuable.

X-ray topographic analysis, to date, not widely used in the analysis of CdTe substrate material, has been shown to yield a wealth of data on defects in CdTe. Resolution can approach 1 μm, sufficient to reveal the lattic strain fields around individual dislocations. Significant structural defect variation in a sampling of CdTe source material was observed, and this could easily relate to variations in epitaxial device performance. A careful correlation between CdTe growth parameters and microscopic defects revealed by topographic analysis would be very valuable, and we propose this as a second, and most important area for further research work.

about each was added to the technical literature.

A most exciting facet of the program is the wealth of data on defects in CdTe, both microscopic and macroscopic, that appears to be available from x-ray topographic analysis, in this case from a synchrotron source. Comparative studies revealed significant stria and subgrain structure in a wide selection of commerical material. Resolution comparable to cathodoluminscence and etching studies has been demonstrated. Widespread slip has been found in a number of sources and may indicate post-growth stress. Localized strain fields, also observed, indicate individual dislocations, dislocation nests, or submicron precipitates. Far more analysis in this area is needed to better correlate microscopic defets with growth parameters.

most microtwins, which are common in CdTe, are thought to be grown-in twins as opposed to annealing twins [18], it seems curious that stacking faults are not evident. In fact, topographic interpretation in highly defective material like CdTe is a relatively new area that is still being developed. Further evaluation of the topographs in hand and additional high resolution studies in low defect material would be valuable. This is the second general area we identify as having excellent potential for further studies.

D. Technical Summary

In summary, this program has been the first broad-ba[illegible] comprehensive study of CdTe vertical Bridgman melt growth parameters. We have accummulated further evidence that low amplitude 60 Hz mechanical vibrations can sometimes lead to nearly single-crystal, low dislocation boules. However, the cause is not yet understood, and the phenomenon has not been optimized to the point of making this a reproducible effect. The widespread inability to grow single crystal CdTe boules on a reproducible basis, indicating poor grain selectivity, is thought to be due to a lack of a strongly preferred growth direction combined with generally flat growth interfaces under all vertical Bridgman growth conditions. This was demonstrated by careful studies of secondary nucleation in CdTe boules and by radiographic interface demarcation using In^{111}.

Preliminary experiments with the heat exchanger method of growth were successful in establishing a convex and presumably more favorable growth interface. Enhanced grain selectivity and significantly improved grain structure appear to be available using this growth technique. Further experiments are needed.

The defect studies in CdTe have been highly successful on two fronts. Chemical etching experiments led to valuable comparative studies of sustrate material from a number of sources. Low defect material grown under 60 Hz vibrations was found occassionally and verified. Attempts to reconcile the etching behavior of the Inoue and Nakagawa etches with etching in the III-V's led us to develop a model which predicts their behavior in the II-VI compounds. New information

these features remains unresolved. This crystal does demonstrate, however, that when near-single boules are obtained from growth under 60 Hz mechanical vibrations, material having significantly reduced defect density is obtained.

Similar effects were found in the In-doped crystals. Fig. 23 (a) shows a reflection topograph from one of these crystals. While some scratch remnants are present, there is much less evidence of striations and subgrain structure. A corresponding etch pit study, Fig. 23 (b), revealed a relatively low etch pit density near $10^4 cm^{-2}$. The mechanism responsible is thought to be a form of solution hardening, and similar results have recently been reported in the $Cd_{1-x}Zn_xTe$ [19], $Cd_{1-y}Mn_yTe$ [10], and $CdSe_zTe_{1-z}$ [21] systems.

An early goal was to determine whether x-ray topography could be used to resolve the question about what kinds of defects exactly does chemical etching reveal, and with what reproducibility. The continuous contrast structure revealed in most of our topographs is strongly suggestive of the subgrain structure shown by chemical etching studies using the Nakagawa solution, Fig. 24. In this reflection topograph of commercial material, individual dislocations cannot be resolved although individual localized dark contrast features can be seen. In this particular case there is close agreement between the size of the subgrains revealed by topography and those revealed by chemical etching. In many cases, finer subgrain structure was revealed by chemical etching than was resolved by topography.

In transmission topography on specimens thinned by chem-mechanical polishing, increased resolution can be gained. In fig. 25 we show diffraction images in which contrast features suggestive of individual dislocations can be seen within the subgrains. We were unable to further analyze these topographs due to time constraints, nor were we able to complete the corresponding etching study of this particular specimen. It is clear, however, that individual dislocations can be resolved and studied by synchrotron topography.

Finally, while the stacking fault energy in CdTe is known to be low compared to other semiconductor systems [5], we have not seen clear features of this type in the topographs we have studied. Since

scopic reflection topographs of our own material that demonstrate the types of defects that were resolved. Lamellar twins split the topographs into two separate images which can be fitted back together to reconstruct the whole image. We show them separated to make more apparent the positioning of the twins. Subgrain boundaries, scratch remnants and surface defects are readily apparent. In Fig. 19a, reflection topographic analysis of a highly defective specimen reveals extensive slip as well as lattice distortion. Chemical etch pit analysis on this same specimen using the Nakagawa etch revealed extensive subgrain structure and an etch pit density near $10^6 cm^{-2}$, Fig. 19b. In Fig. 20, in transmission analysis we observe remnant saw damage extending deep beneath the surface and localized dark areas that could be dislocation clustering or precipitates.

Comparative studies of CdTe from different sources revealed a considerable diversity of defect structure. Samples were obtained from Rockwell International, II-VI, Inc., Fermionics, Inc., Texas Instruments, and Comineo, Inc. (We should caution that it is probably not accurate to assume these particular specimens were representative of their highest quality substrate material.) Reflection topographic analysis, Fig. 21, revealed significant subgrain structure in all cases and slip and stria in most. The frequent occurrence of slip systems in commercial CdTe was somewhat surprising since it had not been revealed previously by other analytical methods. CdTe has been shown to have a low yield stress at elevated temperatures [18] and at tempertures near its melting point, could be quite plastic in character.

In Fig. 22 we show a transmission topograph of a virtually single crystal Stanford-grown boule. This particular boule was grown under the influence of 60 Hz mechanical vibrations, and revealed only minimal subgrain structure and slip. Near the top, it did show localized strain fields (or small dislocation loops). With an infrared microscope having approximately 1-2 μm resolution we were unable to detect any precipitates. Localized strain fields could not be seen with IR microscopy either, probably because of the low extinction polarizers with which these instruments are typically equipped. The cause of

correlation led us to search for additional means to study microscopic defects in CdTe. The method chosen was x-ray synchrotron topography.

2. X-ray Synchrotron Topographic Studies

X-ray synchrotron topography is a non-destructive method suitable for the study of large scale, rather perfect crystals [16]. The x-ray synchrotron source at the Stanford Synchrotron Radiation Laboratory has a beam size of 5 mm high x 10 mm wide and hence Laue topographic images of this size can be recorded. Synchrotron sources are orders of magnitude more intense than rotating anode sources, the beams are highly collimated, and the effective source dimensions are small (in the micron-millimeter range depending on the betatron oscillation amplitude). Exposure times are minimal and diffracted and transmitted-intensities are high so that highly absorbing crystals, like CdTe, exceeding 1 mm in thickness can be studied in the transmission mode. There are no x-ray lenses so that only 1:1 imaging is possible and the resolution is therefore limited to the resolution obtained with nuclear emulsion film which is about 1 μm. The lattice strain fields around individual dislocations in CdTe appear to be substantially larger, so that in principle individual defects can be seen as long as they are not too close together. Typically, individual dislocation can be seen if the total density does not exceed 10^4 cm^{-2}. This coincides with the defect densities in relatively "low d" CdTe. Hence, one should be able to see individual dislocations under optimum circumstances. Larger defects such as precipitates, dislocation tangles, subgrain boundaries, and twin boundaries are readily apparent.

To date only scattered references to the use of x-ray topography to study defects in Bridgman-grown CdTe crystals are found [17]. Because of beam access and time limitations, we were able to complete only a limited number of preliminary experiments during the latter part of this program. The outcome has, however, has been very encouraging, and significant and exciting results have already been achieved. In all the examples to be shown, preparation was by the chem-mechanical polishing technique described in Appendix II and at least 250 μm of surface material was removed. In Fig. 18 we show macro-

have a single dominant grain. In Fig. 16 we show surface etch pit pattern obtained with the Inoue etch, from the edge of the samples and progressing inward to the central regions. In all cases, higher etch pit densities were observed on the edges than in the central areas as anticipated. Typical numerical densities are shown. In the Stanford material, we found a large central area which was essentially free of etch pits. This area did not pit with repeated etching and polishing. Not all boules grown under the influence of 60 Hz mechanical vibrations were "low d," but when crystals were virtually single, low etch pit densities were usually found.

Because the Nakagawa etch works only on the [111]A faces it was significantly harder to use for characterizing large cross-sectional slices. In the limited work we did carry out by orienting and sectioning the largest grain in a boule, not such a clear distinction between various samples was observed. Nor did we observe a strong correlation with vibration. The total number of boules studied with the Nakagawa etch was probably too small to be statistically significantly, however.

Confidence in the comparative value of the Nakagawa etch was obtained from EPD studies on one of the In^{111}-doped boules. Anticipated dopant incorporating levels were in the 10^{18}-10^{20} cm^3 range. Cross-sectional studies revealed average etch pit densities of ~1.7 x $10^4/cm^2$ as compared to an average of 10^5-$10^6/cm^2$ for an undoped boule, Fig. 17. This behavior is expected on the basis of solution-hardening and has also been documented in the $Cd_{1-x}Zn_xTe$ system by Bell and Sen [13].

The most we can conclude about our CdTe boules at this point is that in a percentage of 20 mm dia. boules grown under 60 Hz mechanical vibrations, large virtually single crystal regions are found which tend to yield very low etch pit densities.

One problem with chemical etching studies is that no one has yet demonstrated a 1:1 corespondence between chemical etch pits and the various types of dislocations that are known to form in CdTe, although Chin [14] and Bubulac, et al. [15] have shown a correspondence between cathodoluminscence and etch pits by Nakagawa solution. This lack of

ed to be related to thermal stresses around the quartz fusion joints. The ingot was retrieved in fairly good conditions with the exception of some cracking and evaporative losses near its top. The grain structure was revealed by sectioning and a schematic reconstruction is shown in Fig. 15. In general, the initial selectivity appeared to be excellent, minimal secondary nucleation from the walls was found, and only a modest amount of lamellar twinning was observed compared to 28 mm dia. boules. From a growth ampoule design that was obviously far from optimum, these results are considered very promising. This is one area that seems promising for continued research.

C. Analytical Studies of Defects in CdTe

1. Chemical Etching Studies of Defects in CdTe

Considerable attention has been devoted in this program to the development of reliable chemical etching techniques for the analysis of dislocation densities in CdTe. One of the problems at the time the program began was that there was little faith industry-wide in chemical etch pit density measurements. They tended not to be reproducible and to give considerably lower numbers than those arrived at by TEM analysis. Our emphasis was to develop a reproducible method in-house so that accurate comparison studies could be made. Two common etches were used in this work: those developed by Inoue [1] and the one developed by Nakagawa [2]. This work was generally quite successful and new knowledge on the behavior of both etches was added to the literature in a second refereed publication, "Etch Pit Studies in CdTe Crystals." We include this manuscript in Appendix II.

In general we found that these two classes of etches never produced similar results (the Nakagawa etch always produced a significantly higher density of etch pits by a factor of $10\text{-}10^3$) but that both seemed to behave reproducibly when used to compare one sample of CdTe against another.

Several comparative studies were carried out. In the first, we compared large cross-sectional slices obtained from II-VI, Inc.; Rockwell International; Fermionics, Inc.; and one of our own boules grown under the influence of 60 Hz mechanical vibrations, which happened to

decrease in the furnace temperature. Melt-solid interface shapes generated by this technique should be convex at all times because of the quasi-hemispherical symmetry as shown in Fig. 12.

Considerable effort was invested in constructing a 50 mm dia. sealed quartz growth ampoule with five reentrant fine thermocouple wells, Fig. 13. The thermocouple wells were incorporated to allow continuous melt probing with Pt-Rd thermocouples to determine the exact shape of the isotherms and consequently the shape of the growth interface.

An extended experiment to carefully determine the in-situ thermal distributions as a function of furnace set point and cooling gas flow-rate was carried out in one of the tubular furnaces set up with an isothermal profile. The mass of the CdTe charge used was approximately 600 g. Thermal data was collected manually and reduced by both computer-aided numerical reduction and by graphical methods. Only one extended thermal analysis experiment was carried out due to the conclusion of the program, and we were able to only partially complete it before a failure in the quartz ampoule occurred. The results obtained, however, were excellent and verified that we had successfully achieved a convex growth interface shape. In Fig. 14 we show a composite analysis which contains four thermal profiles which were measured at radial positions corresponding to the four dashed lines. Four separate temperature scales were used and each was positioned such that the melting temperature of CdTe (1092°C) fell exactly on the coresponding dashed line. The intersections of the four thermal profiles with the four dashed lines then revealed the position of the melting point isotherm along the dashed lines, and these in turn revealed the shape of the growth interface for that particular set of thermal data.

We were able to verify the convex shape of the growth interface only in the bottom third of the ampoule before the quartz failure occurred. Nonetheless, the results were highly encouraging and a crystal growth experiment without thermocouple wells was carried out to take a preliminary look at grain selectivity in the HEM configuration. This experiment, too,experienced a quartz failure which appear-

felt that stronger localized cooling and a more favorable growth interface shape should occur with this type of ampoule, and explain the strong initial grain selectivity observed in our growth experiments. Radiographic interface demarcation experiments in the flat-bottomed geometry were inconclusive, however, due to lack of resolution at the bottom end of the growth ampoule and the apparent incorporation of a large quantity of In^{111} in the first-to-freeze material at the very bottom of the ampoule. Growth interfaces more than 1 cm above the bottom were essentially flat as before.

To further ellucidate the shapes of the growth interface in flat-bottom growth ampoules, a qurtz ampoule having two reentrant fine thermocouple wells was constructed. One thermocouple well was positioned along the axis, and the second was parallel to this but near the side of the ampoule. Fine Pt-Rd thermocouples were used to continuously profile the melt/solid temperature distributions during growth. The vertical position of the growth interface (T_{mp} = 1096°C) was carefully noted, both on-axis and off-center. This allowed a two-point determination of the growth interface curvature. In general, we verified flat growth interface shapes occurred within the main body of the ampoule. Within 5 mm of the bottom, slightly convex interface shapes were found, which seemed consistent with our observation of effective grain selection there.

4. Control of Growth Interface Shapes Using the Heat Exchanger Method

In order to carry out a more definitive study on the interface shape effects, a radically different approach was chosen to create continuously convex interface shapes during the entire growth interval by using the technique known as the Schmid-Viechnicki method, or the heat exchanger method [12]. In this technique a growth ampoule of relatively square aspect ratio is seated on a central localized high temperature heat exchanger. The growth ampoule is heated in an isothermal furnace, and unidirectional solidification is forced to occur radially outward from the heat exchanger by a combined programmed increase in the heat exchanger cooling gas and by a programmed

Vapor phase evaporation and recondensation of CdTe near its melting point have been observed by Kuwamoto [9] who was able to minimize their effect on seed attachment in a vapor transport system by the use of an inert ambient during warmup. Inert gas backfills did not seem to have a significant effect in our melt growth experiments.

3. Determination of the Melt/Solid Growth Interface Shape

The preceeding studies on the effects of growth parameters and seed orientation, and the behavior of secondary grains all suggested a poor grain selection mechanism which as stated previously is commonly held to be related toan unfavorable growth interface shape. Studies were therefore undertaken to unambiguously reveal the growth interface shapes under a variety of growth conditions. Interface demarcation by the use of In^{111} as a radiotraceable dopant, following the early work by Kyle [10], was selected, and a series of experiments was carried out in the conventional Bridgman growth ampoule geometries. This work was recently published in a refereed journal and is included in its entirety as Appendix I.

In summary these experiments revealed relatively flat interface shapes in all cases. This was thought to be consistent with our observations of poor grain selectivity. Enhanced gradient experiments were carried out to produce a more favorable (convex) interface shape, but even with forced seed cooling and additional gradient-enhancing booster heaters, we were only able to produce slightly convex interface shapes. Metallographic sectioning of these boules did not indicate a significant improvement in grain structure. A converse experiment to generate unfavorable concave growth interface shapes also yielded relatively planar interfaces. This has led us to conclude that it is, for fundamental reasons, difficult to modify CdTe growth interfaces in the usual cylindrcal tube furnace geometry because of the low thermal conductivity of both the melt and the solid, and a high effective Biot number in the CdTe system [11].

Flat-bottomed 28 mm ID growth ampoules having no grain-selecting capillary at all were analyzed next. Because of the comparatively strong radiative coupling factors in high Biot number systems, it was

events were found to occur at the edges of the boules and subsequently work in, although occasional grains nucleating in the interiors of the boules were found as well. This relatively poor grain selectivity effect was highly suggestive of a possible unfavorable growth interface shape. {It is commonly held that concave interface shapes are unfavorable because they promote the inward growth of surface nucleated defects, whereas convex interface shapes are favorable because they promote the outward growth of surface nucleated defects [6]. We show this schematically in Fig. 9.} A flat interface shape in a material like CdTe which does not have a strongly preferred growth axis could result in poor grain selectivity.

2. Effects Due to growth Ampoule Geometry

In plotting the number of grains per cross-section along the lengths of several boules grown in conventional Bridgman geometry ampoules, secondary nucleation was found to occur primarily in the flare-out region, and thereafter in the main body of the boule, grain selectivity was weak, Fig. 10. This was again thought to be consistent with an unfavorable growth interface shape. From a consideration of the heat flow across the growth interface, one expects the most concave shape to occur in the conical region [7, 8].

To ellucidate this effect, a number of flat-bottom ampoules were constructed which had no seed pocket or conical section. In the first self-nucleated growth experiment, we were surprised to find that the initial grain selectivity was very effective. The number of grains per cross-section dropped from an initial value near one thousand down to two within the first 4 cm of growth (Fig 11a-c). Thereafter, the two grains persisted. Attempts to use this bicrystal as a full cross-section seed for subsequent growth experiments were only partially successful. While a clean melt attachment was achieved after several trials, subsequent grain selectivity was poor and secondary grains appeared immediately on the sides of the boules. This was a commonly observed phenomenon, where self-nucleated boules grown from a significantly more superheated melt exhibited less secondary nucleation than cases where superheating was limited due to the presence of a seed.

ture but not significantly.

We also found that the same 60 Hz vibrational parameters that were highly effective in the 18 - 20 mm dia. size boules used in our previous studies were far less effective at reducing grain structure in 28 mm dia. boules. This is not particularly surprising: we anticipated that in the larger, more massive boules, some "tuning" of vibrational frequency and amplitude would be necessary to accomplish the same degree of statistical improvement. Due to the earlier than anticipated conclusion of this program as discussed in Chapter I, we were unable to pursue this area of interest.

None-the-less, some other fundamental factors seemed to be at work and further analytical studies were undertaken.

B. Analytical Studies of Structural and Growth Parameters

1. Grain Structure in CdTe Boules

In typical CdTe boules, one finds several types of boundaries: simple twins, lamellar twins and non-planar incoherent boundaries as shown in Fig. 7. Two types of curved boundaries are shown, one is a truly random grain boundary but the second is a twin boundary where two or more successive 180° rotational twinning events occur; first about a [111] and then about a [111], resulting in a curved, apparently incoherent boundary where the parent grain meets the second and higher order twins. This type of twinning has been found in silicon by a number of authors, but has also been reported in compound semiconductors [4]. A substantial fraction of the curved, apparently incoherent boundaries that we have observed in CdTe appeared to be higher order twins rather than randomly nucleated grains. This seems consistent with Mooser and Pearson [5], who report that CdTe has a very low stacking fault energy compared to typical III-V compounds. Consequently, one might expect to see more stacking faults and twinning accidents during growth as compared to true secondary grains.

To determine where the twins and secondary grains were nucleating, several boules were fine-sectioned using a wire saw and then each section lightly ground and inspected for structure. A typical sequence of cross-sectional slices is shown in Fig. 8. Most secondary

down, crystal quality was essentially the same as self-seeded boules. An orientation study of the most dominant grains in these polycrystalline boules, Fig. 5, did reveal that they tended to cluster near the <110> - <210> direction. Consequently we used the <110> as a favorable seed orientation for further evaluation of growth parameters.

In all, we evaluated the influence of growth rate, thermal gradients at the growth interface, inert gas backfill, the presence or absence of 60 Hz low amplitude mechanical vibrations, and periodic regrowth. Growth ampoule shapes were also varied and this will be discussed at length in a subsequent section. The range of parameters varied is also shown in Table I.

(Periodic remelting has not been used to any significant degree in Bridgman melt growth of compound semiconductors, however, it has been shown by Jackson and Miller [3] to greatly enhance grain selectivity in some crystal systems. An evaluation was, therefore, included in this work.)

4. Structural Characterization

Structural characterization of the CdTe boules was carried out primarily by sectioning and fine grinding. With a finely-ground surface the gross structural features in CdTe are quite visible to the eye. Abrasive polishing and chemical etching with HF: 2(20gCrO_3 + 100g H_2O) were also used to reveal finer structural details such as small grains and finely spaced lamellar twins.

5. Results of Growth Parameter Studies

No really strong correlation was observed between any of the growth parameters studied and boule structure. In general, almost all boules grown in conventional Bridgman ampoules, independent of initial seed orientation, experienced secondary nucleation and grew as large-grain polycrystals which contained an average of 2-3 grains in an average cross-section. In Fig. 6, we show typical boule cross-sections of a number of boules grown under varying growth conditions. Periodic regrowth did appear to offer some reduction in grain struc-

TABLE I

Number of Experiments	Most Significant Parameter Studied
3	Learning to effect reproducible seed attachment
10	Effects of seed orientation
16	Effects of other growth parameters such as thermal gradients, growth rates, periodic remelting, low frequency mechanical vibrations
9	Growth interface demarcation by radiotracer method
3	In-situ thermal profiling to control growth interface shape
5	Comparative study of low frequency vibrations on dislocation densities
45	**Total Crystal Growth Experiments**

TABLE II

Growth Parameter	Range of Variable
Seed orientation	[111], [110]*, [210], [100]
Thermal gradient at growth interface	2.5, 10†, 18°C/mm
Growth rate	0.3, 1.0*, 3.0 mm/hr
Periodic regrowth	0.5, 1.0 mm/hr 1, 60 min period with 50-75% remelt
Growth ampoule shape	Normal Bridgman with 8 mm^2 seed pocket, 28 mm dia; flat bottom with no seed pocket, 30 mm dia.
Inert gas backfill	†,0 0.5 Atm Argon
Low amplitude 60 Hz mechanical vibration	0.0, 0.005 g*

* most favorable

† nominal

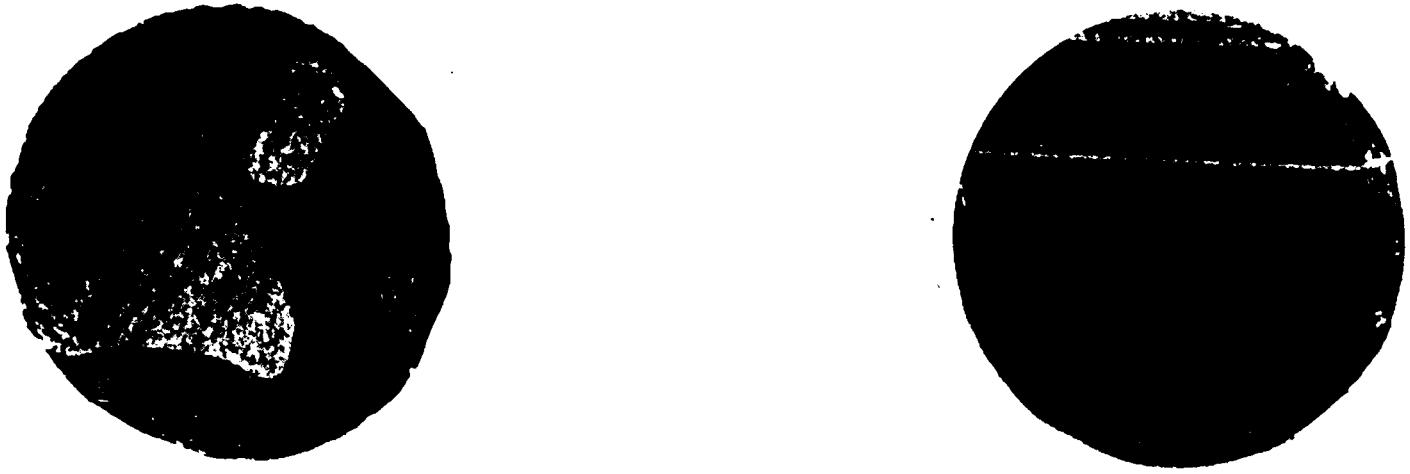

(a) (b)

Fig. 1. Cross-sections of typical CdTe Bridgman boules (18 mm dia.) grown (a) without and (b) with the application of low amplitude 60 H_z mechanical vibrations. Vibrational acceleration was measured to be 0.01 g peak-to-peak.

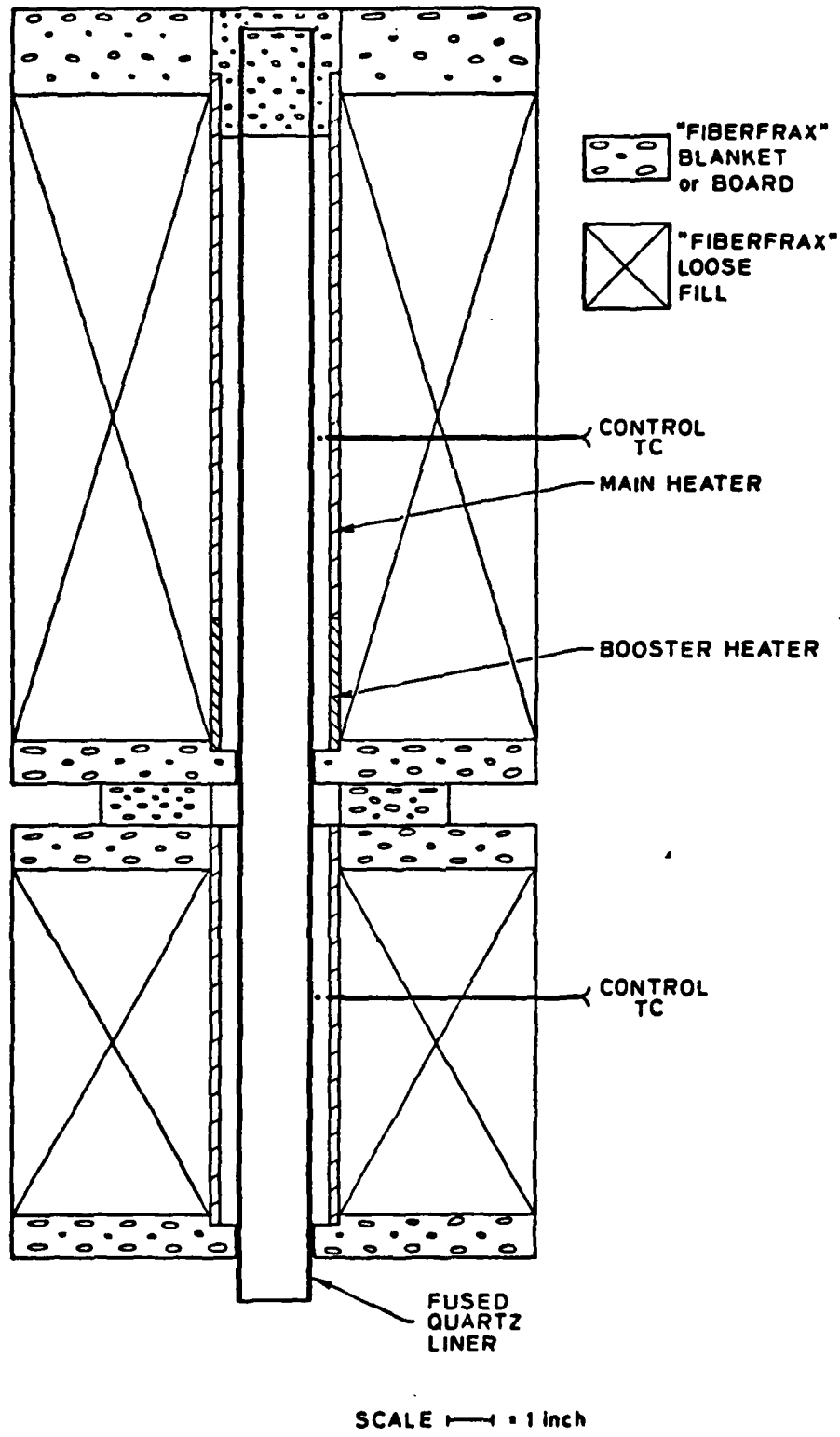

Fig. 2(a). Construction diagram of 2.5" ID Bridgman furnace with booster heater.

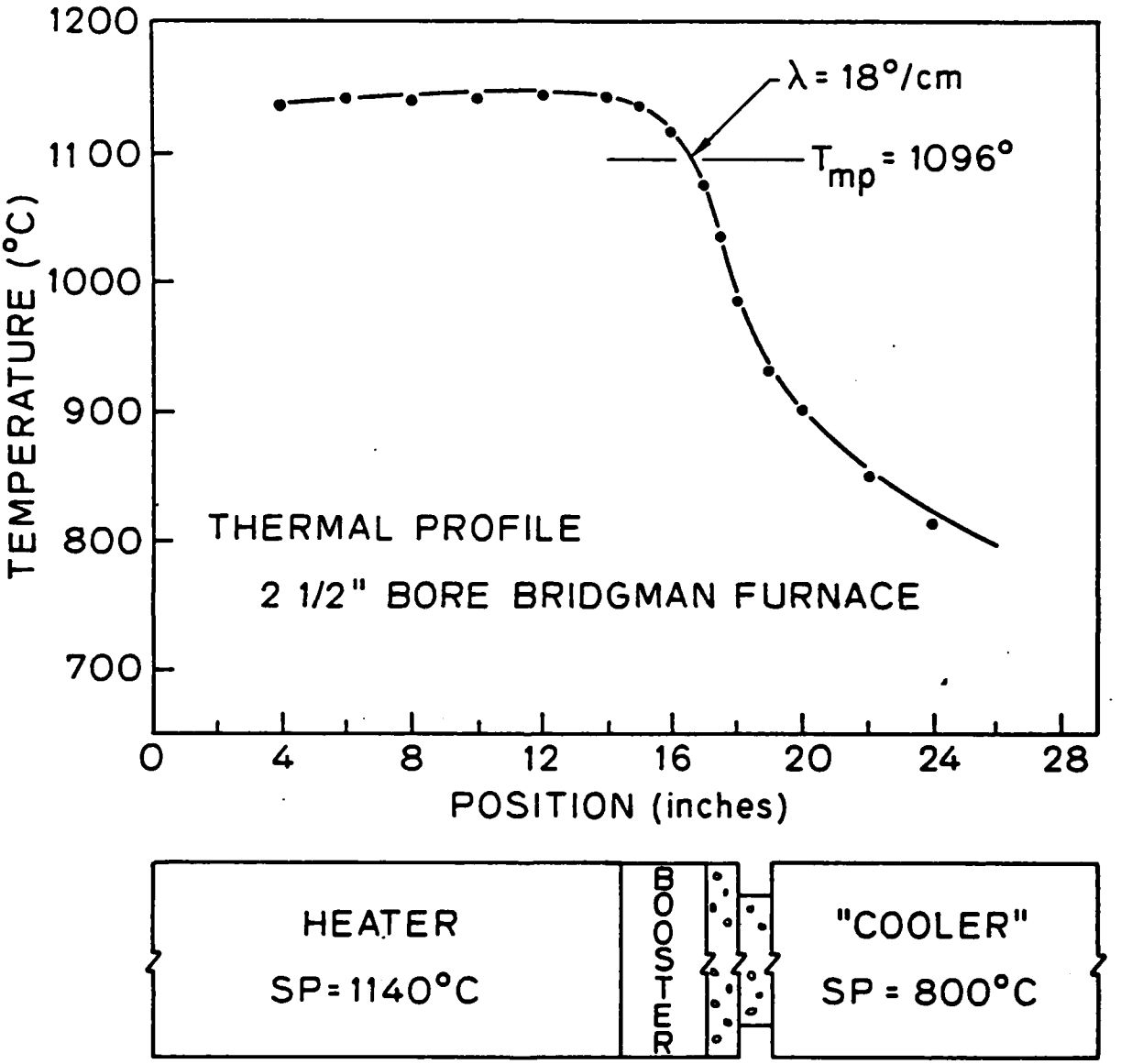

Fig. 2(b). Typical temperature profiles in Bridgman furnace. Nominal temperature gradient at the melting temperature of CdTe (1096°C) was 18°C/cm.

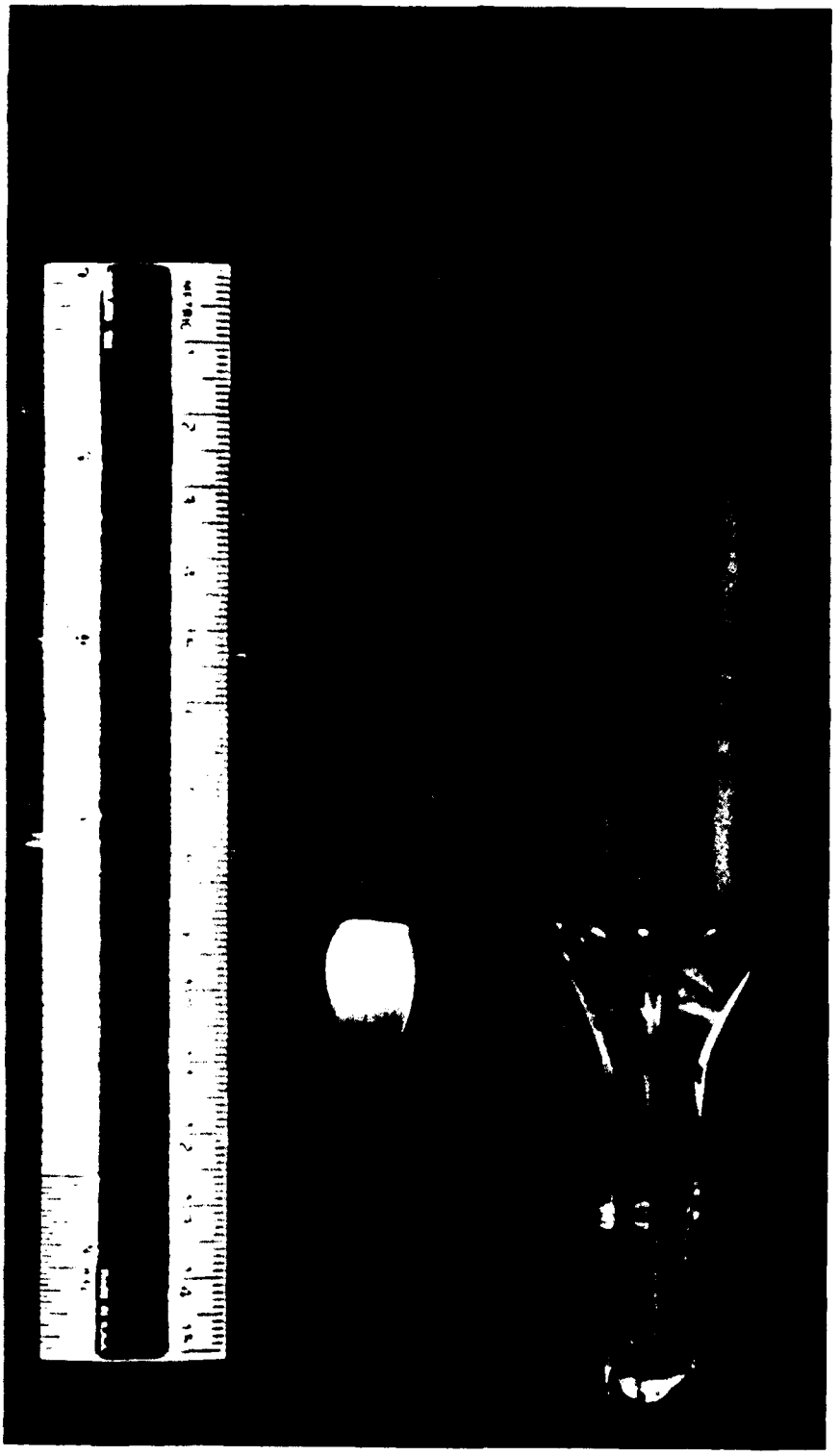

Fig. 3. Vacuum-formed quartz growth ampoule together with precision-tapered carbon mandrel.

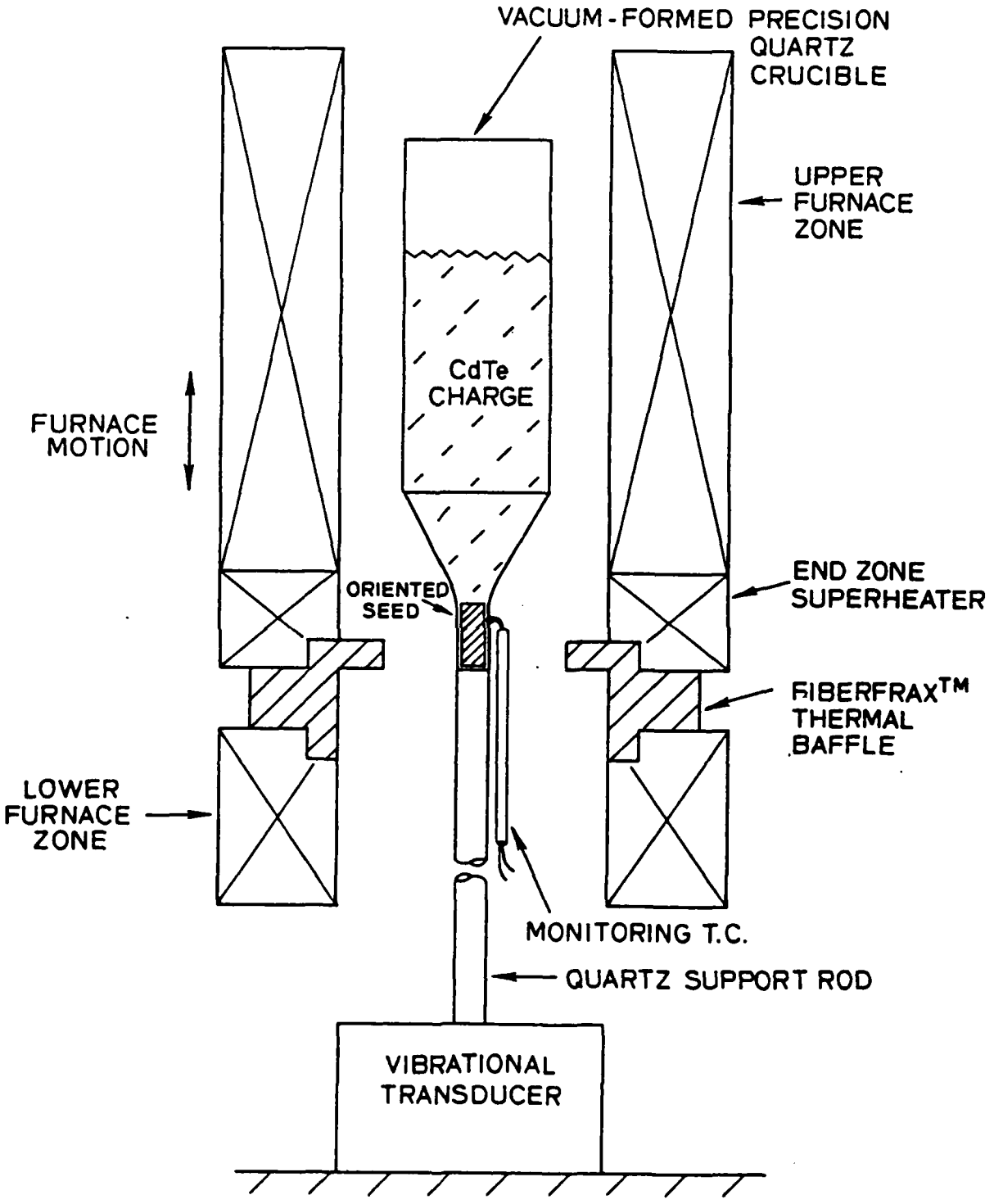

Fig. 4(a). Growth system schematic showing vibrational transducer and technique used for controlled seed meltback.

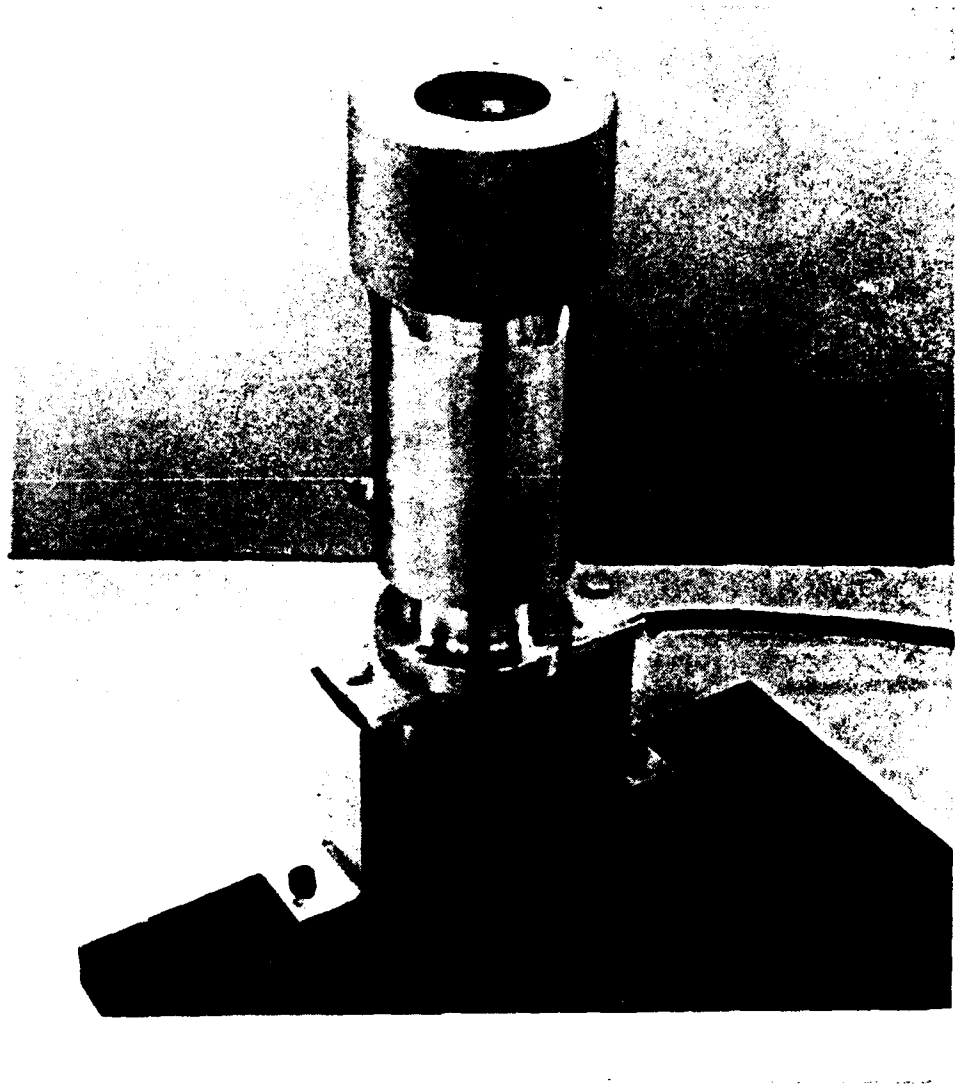

Fig. 4(b). Photograph of vibrational test fixture and coupling chuck (35mm ID) to hold crucible support tube.

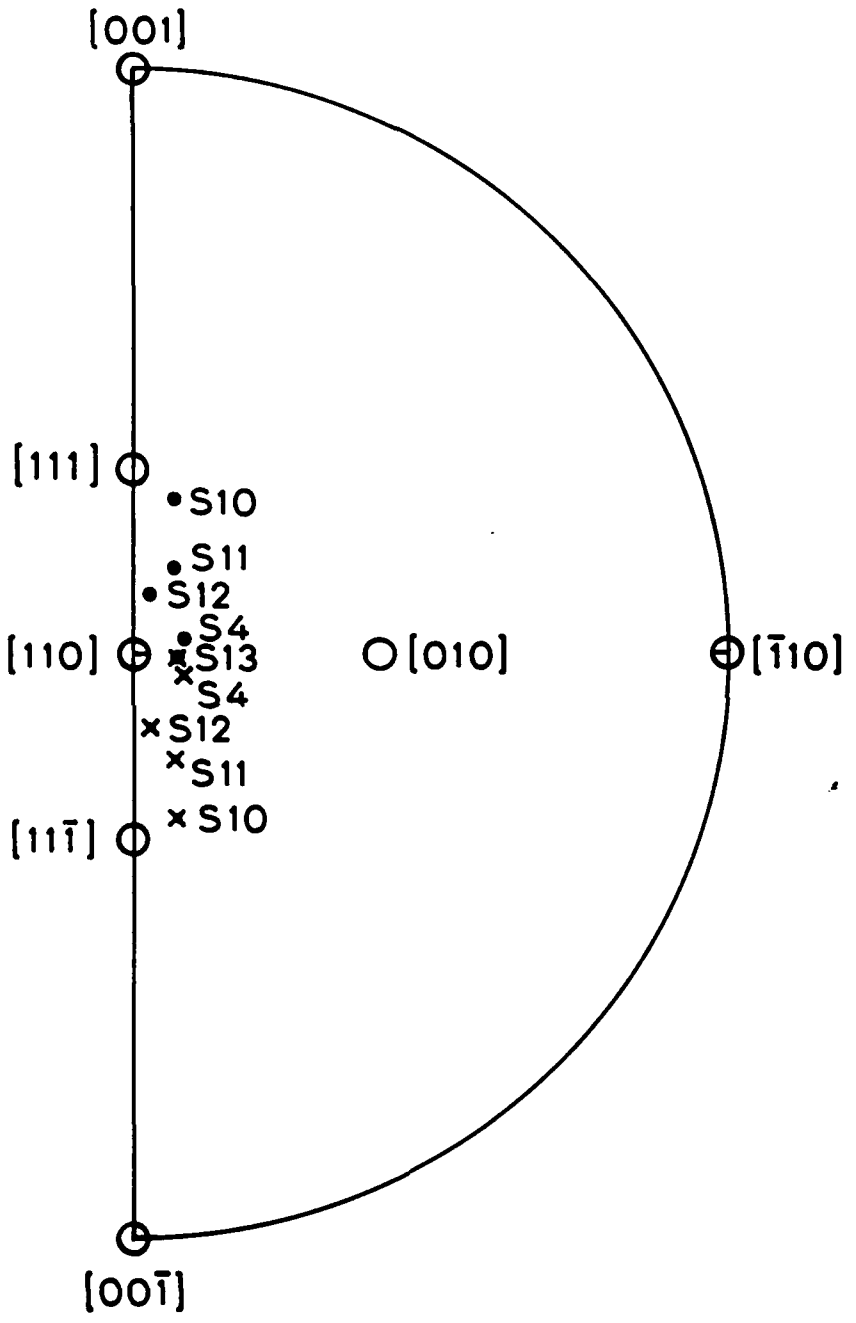

Fig. 5. Stereographic analysis of the growth orientation of the dominant grain in several polycrystalline CdTe boules. Independent of polarity, which was undetermined, clustering was near the [110] - [210] direction, and this growth direction corresponded with boules having the best grain structure.

Fig. 9 Longitudinal cross-sections of a selection of CdTe boules grown under a wide range of growth parameters. a) - d) show effects of seed orientation along [100], [110], [111]A, [111]B respectively. Growth rate dependence at: e) 1/3 mm/hr., b) 1 mm/hr, and f) 3 mm/hr. Periodic regrowth at net 1/2 mm/hr with 'no' melt-back showing also the lack of variation in grain selectivity with boule length g) and h). All crystals were grown under otherwise nominal growth parameters.

STRUCTURAL FEATURES

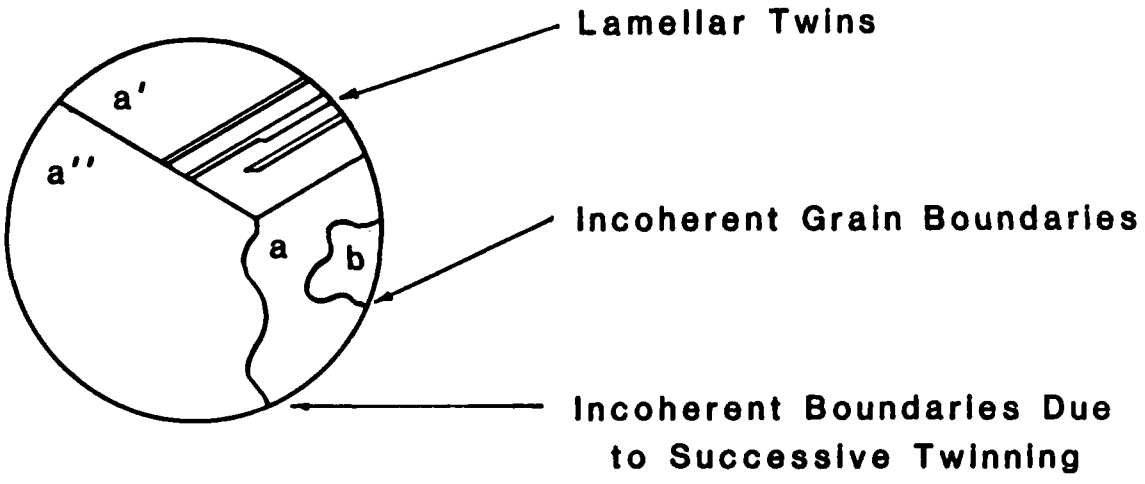

Fig. 7. Structural features seen in typical polycrystalline CdTe boules.

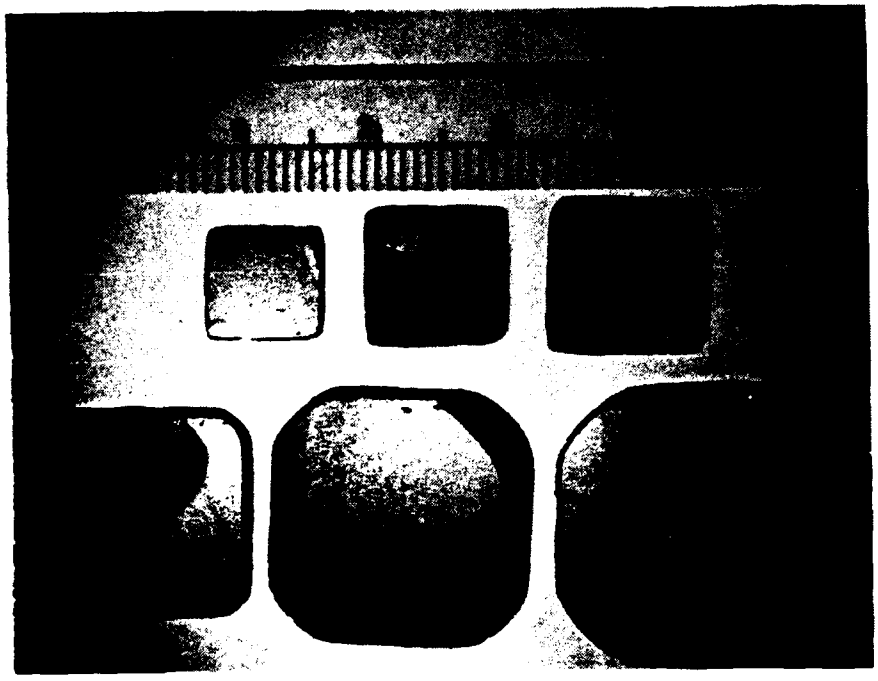

Fig. 8. Cross-sectional slices from the seed, through the flare-out region, up to the begining of the main body of the boule. The seed, except for one minor lamellar twin, was otherwise single crystal. Major breakdown occurred in the flare-out region.

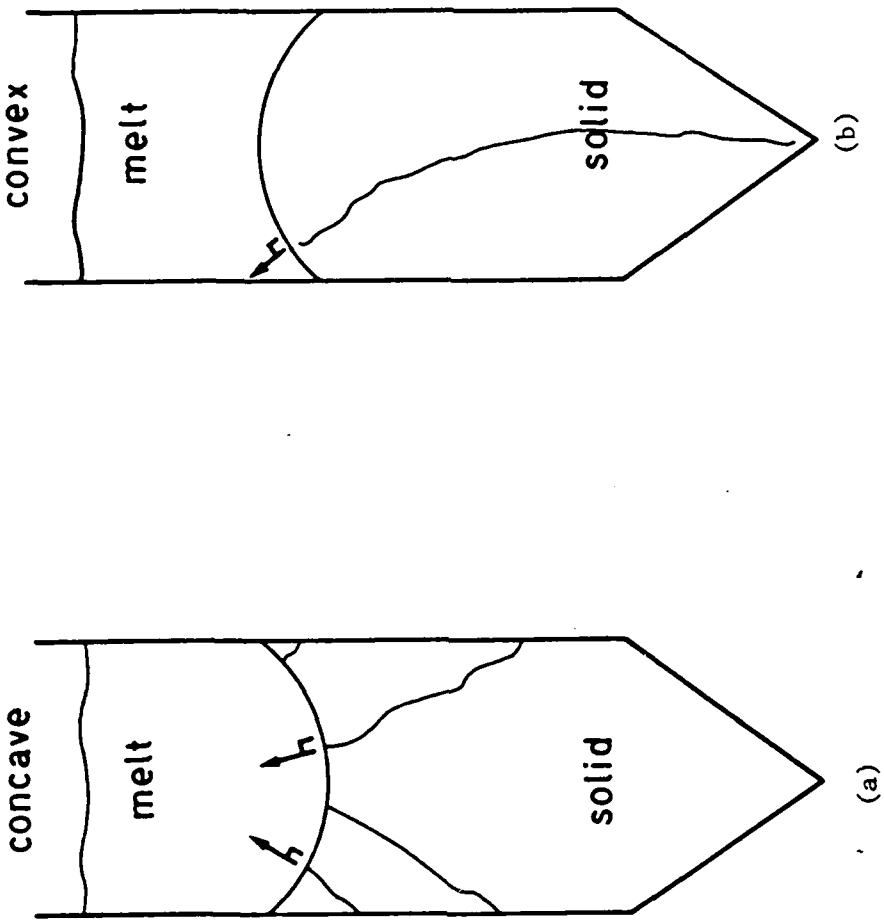

Fig. 9. Schematic diagram showing effect of interface shape on grain selectivity. a) A concave interface shape promotes growth inward of surface defects. b) A convex interface shape promotes growth outward, instead.

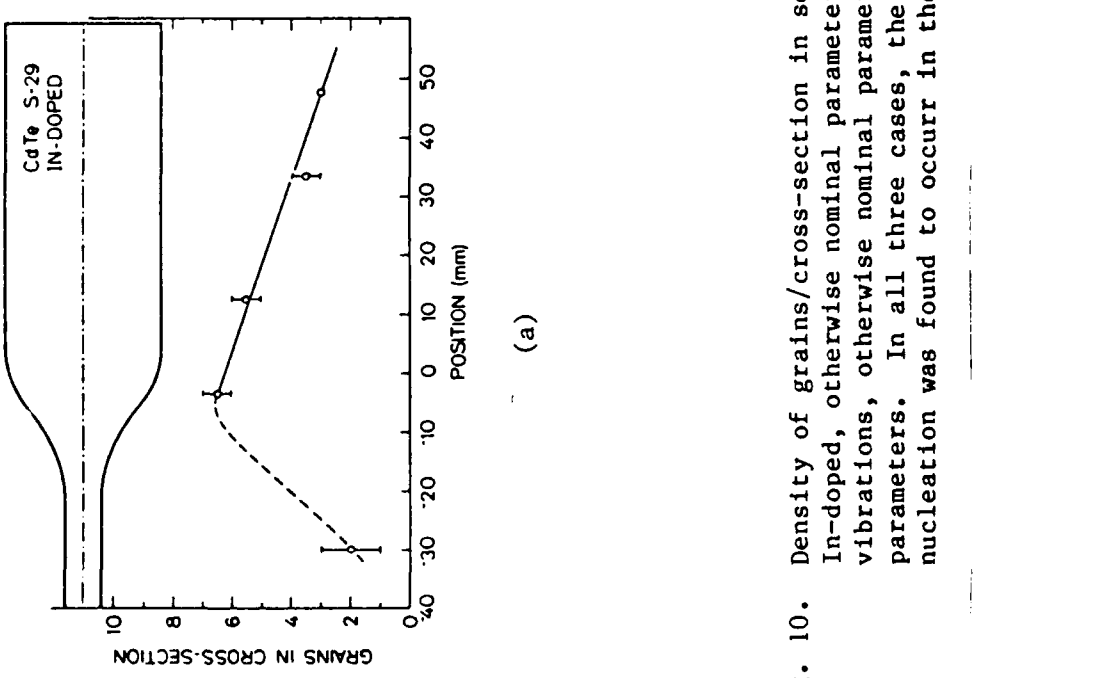

Fig. 10. Density of grains/cross-section in several boules. a) In-doped, otherwise nominal parameters; b) no melt vibrations, otherwise nominal parameters; c) nominal parameters. In all three cases, the bulk of the secondary nucleation was found to occurr in the flare-out region.

Fig. 22. Transmission topograph of a Stanford boule grown under the influence of 60 Hz mechanical vibrations. Almost no subgrain structure or slip is seen. The identity of the dark contrast localized features is unknown: they did not appear under IR microscopic examination and hence are probably not precipitants. [Millimeter scale]

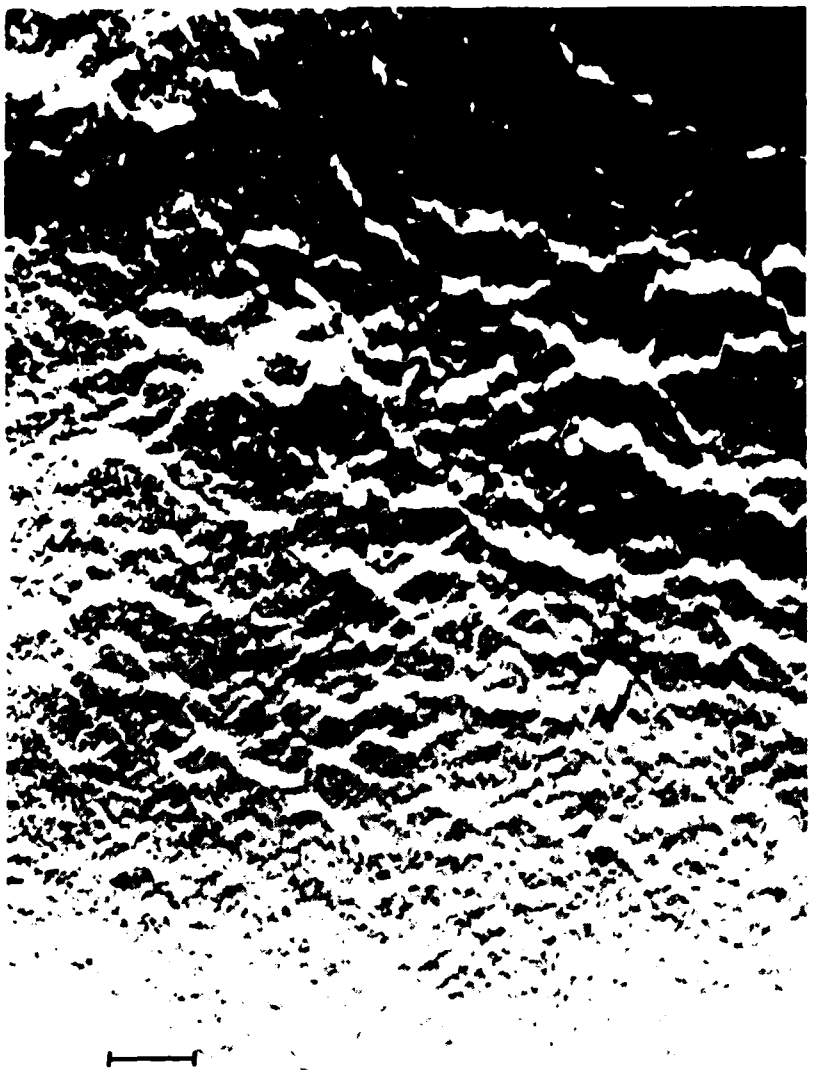

(d)

(e)

Fig. 21 (continued)

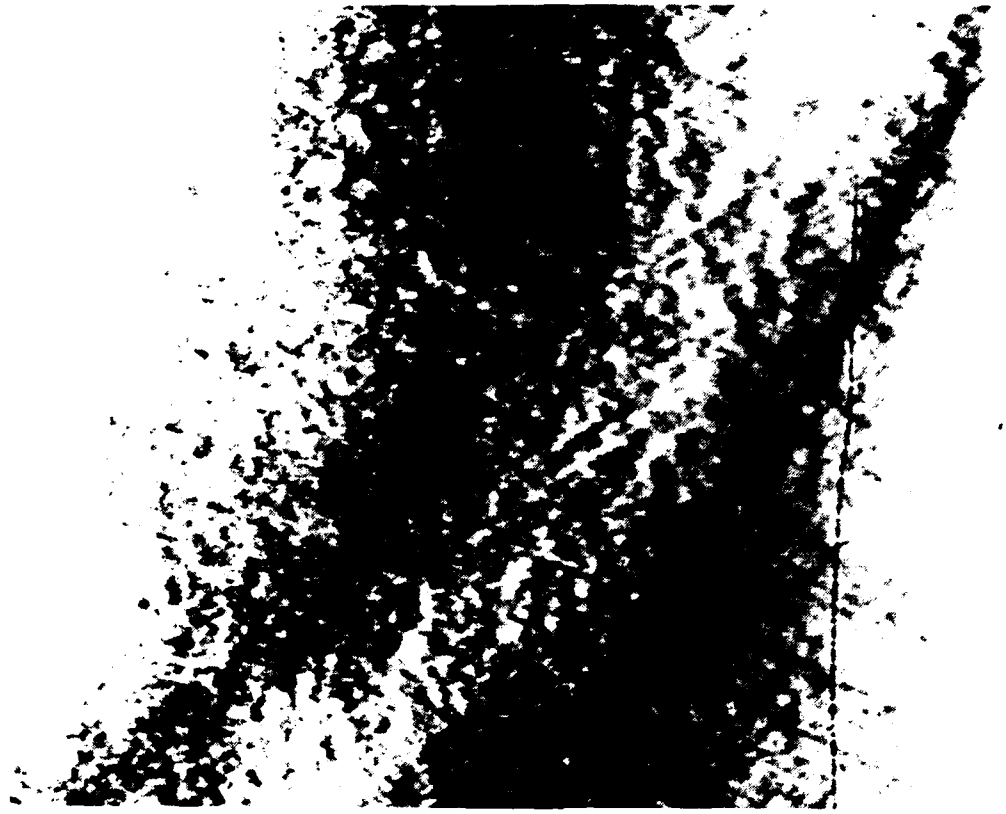

(c)

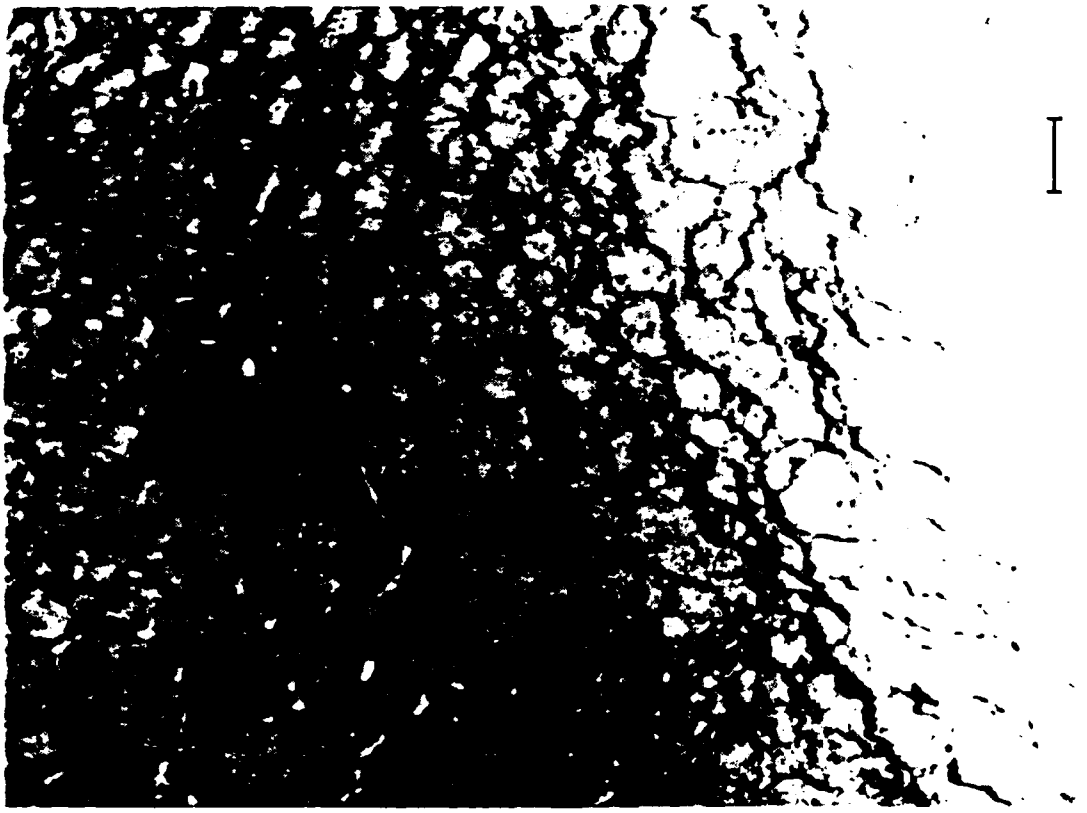

(b)

Fig. 21 (continued)

(a)

Fig. 21. Topographic study of commercial CdTe substrate material from five different sources: (a) - (d) reflection analysis, (e) transmission analysis. All reveal extensive subgrain structure. (a) - (c) reveal extensive slip as well. [Millimeter scale.]

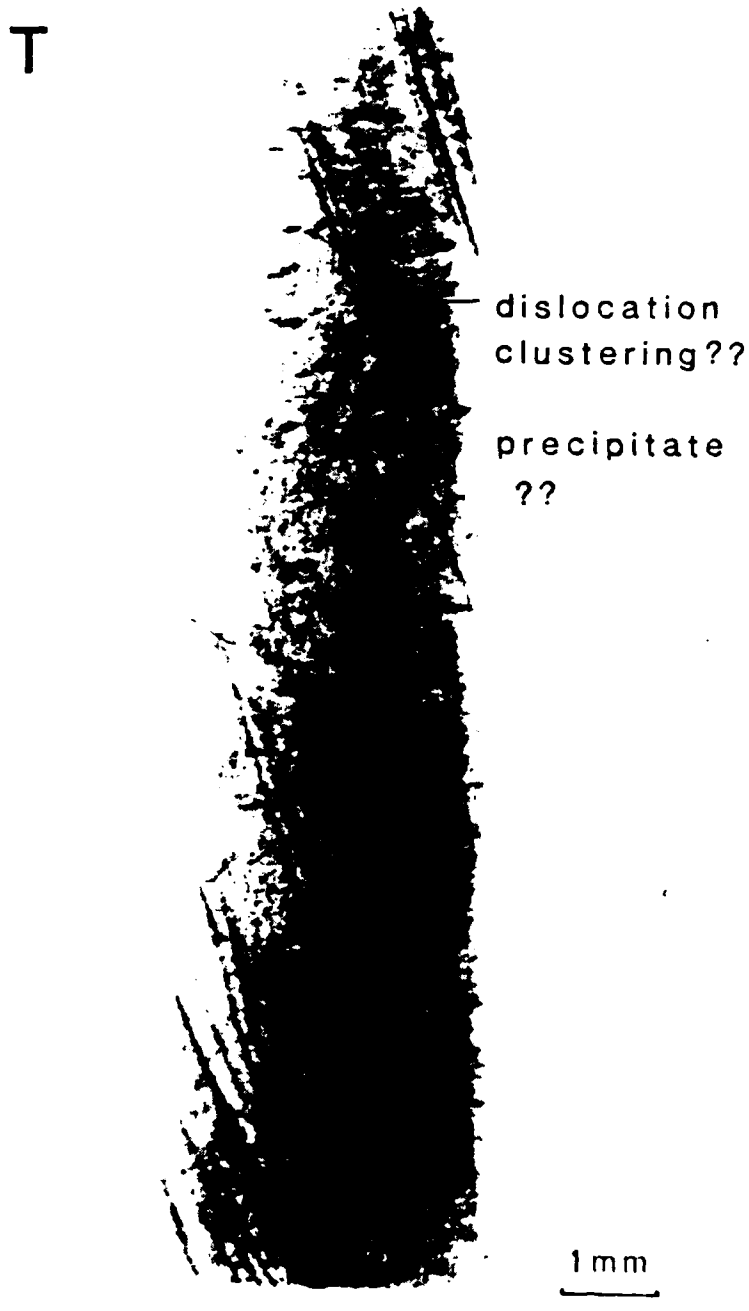

Fig. 20. Transmission topograph of one of our own undoped crystals reveals remnant saw damage deep beneath the original surface as well as localized dark areas that could be dislocation clustering or precipitates.

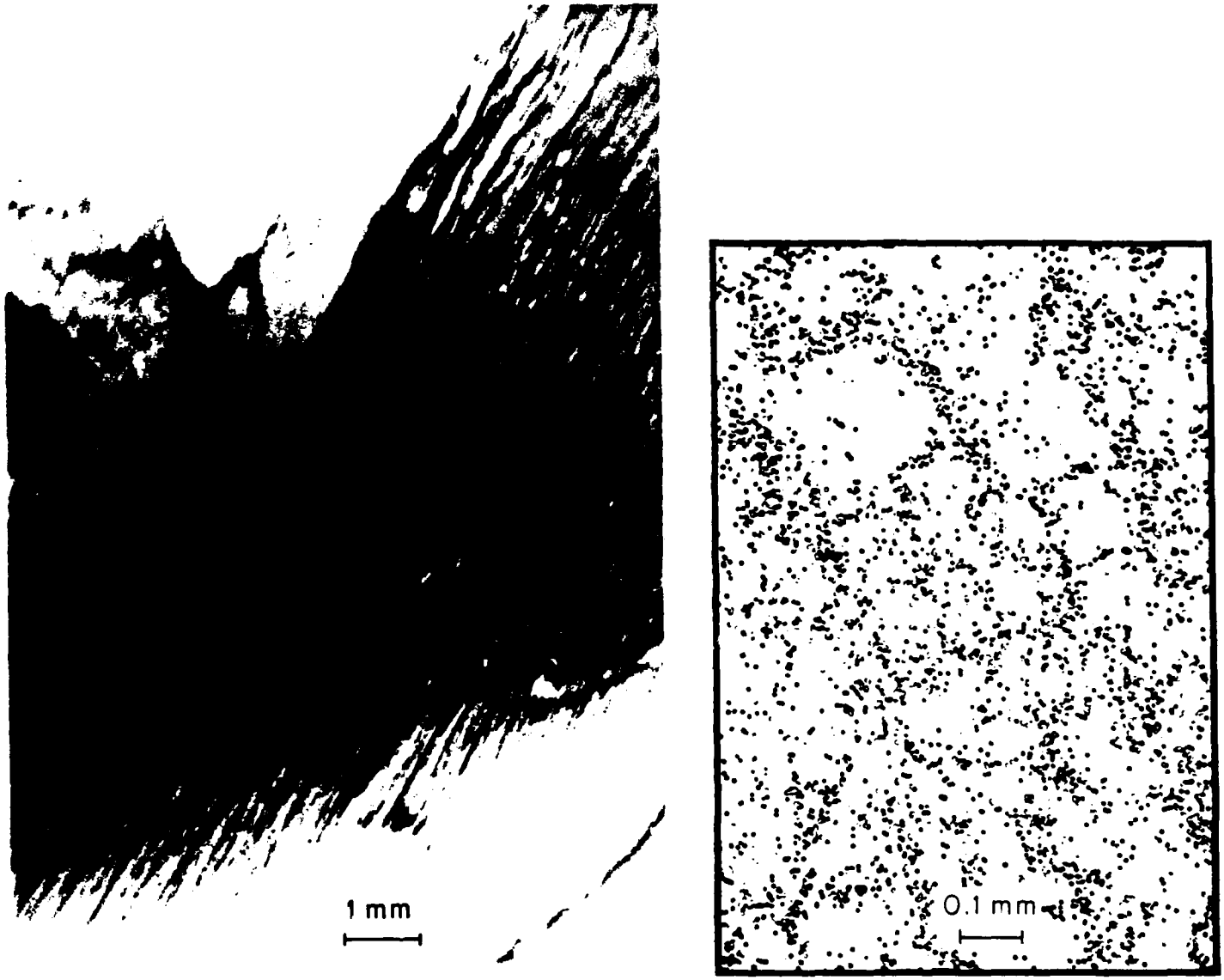

(a) (b)

Fig. 19. (a) Reflection topograph of high defective CdTe which reveals extensive slip. (b) Corresponding etching study reveals extensive etch pitting, and considerable fine subgrain structure. EPD = $10^6 cm^2$ by Nakagawa solution.

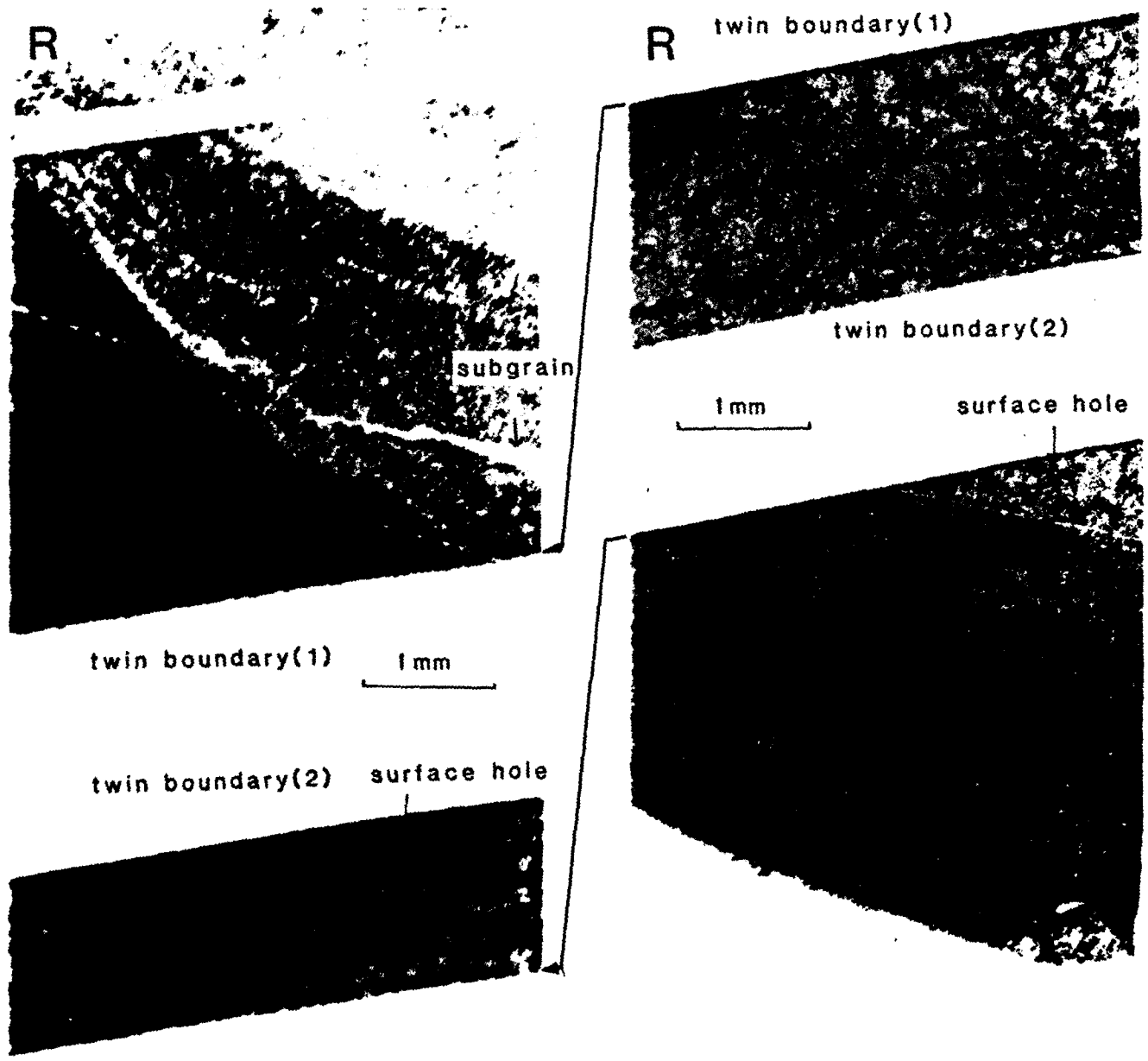

Fig. 18. Reflection synchrotron topograph of a Stanford-grown CdTe control boule. The two images on the right correspond to the two out-of-contrast segments on the left. Subgrain structure and individual dark contrast defects are evident (upper right and lower left). EPD = 7×10^4.

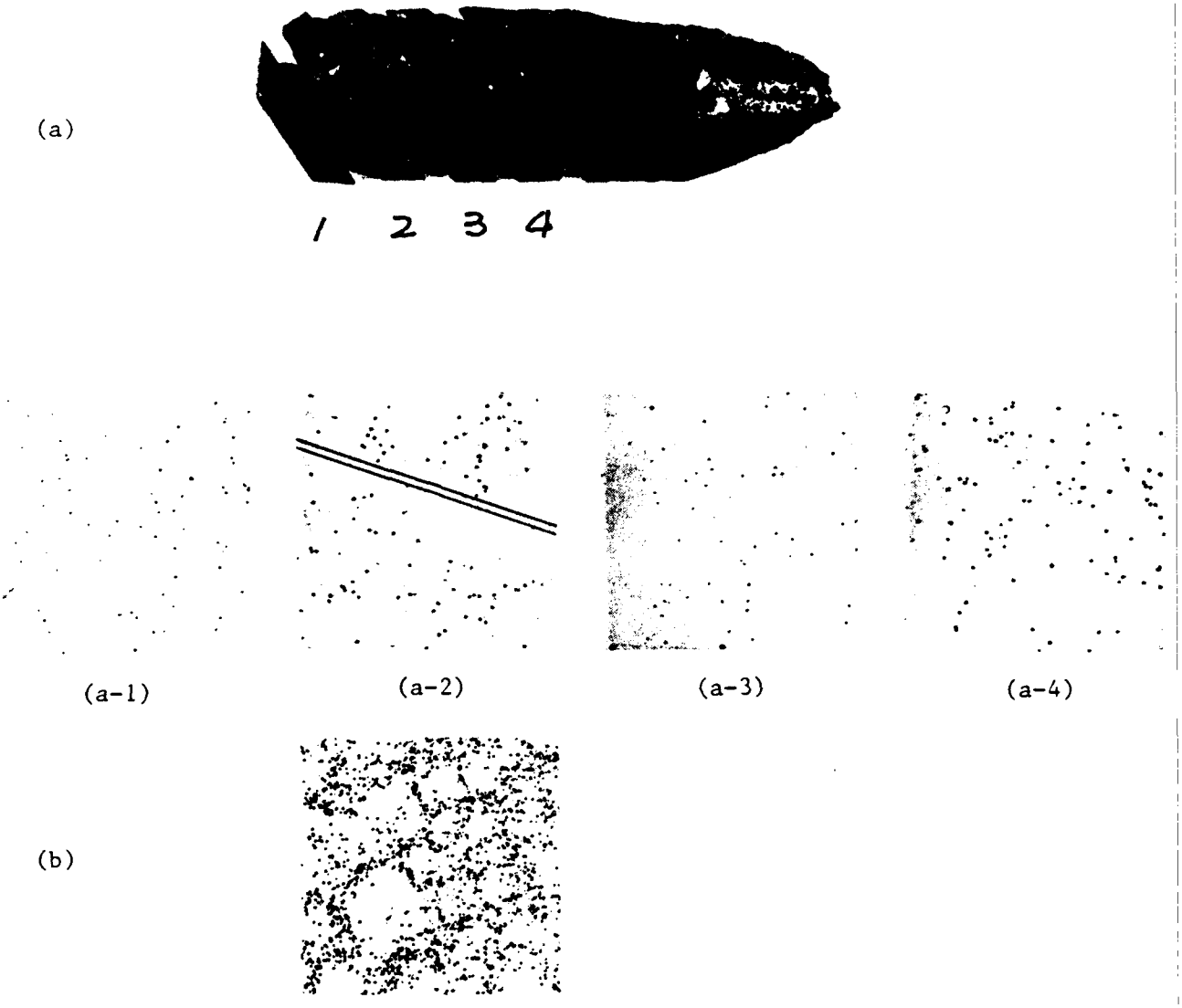

Fig. 17. Etch pit studies on In-doped CdTe boule using "Nakagawa" etch. Average etch pit density in four oriented sections (a-1) - (a-4) was found to be 1.7×10^4 cm^{-2}. By comparison, typical densities in undoped, highly defective boules are in the 10^5 - 10^6 cm^{-2} range, (b). Scale 50X.

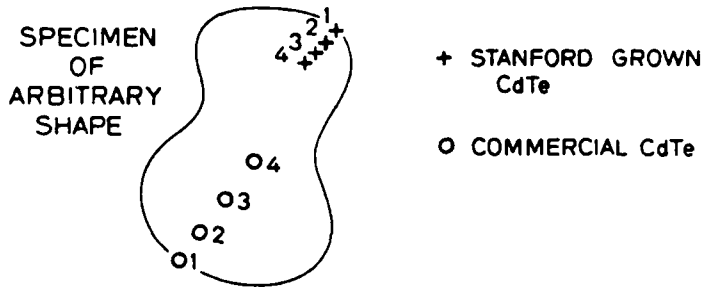

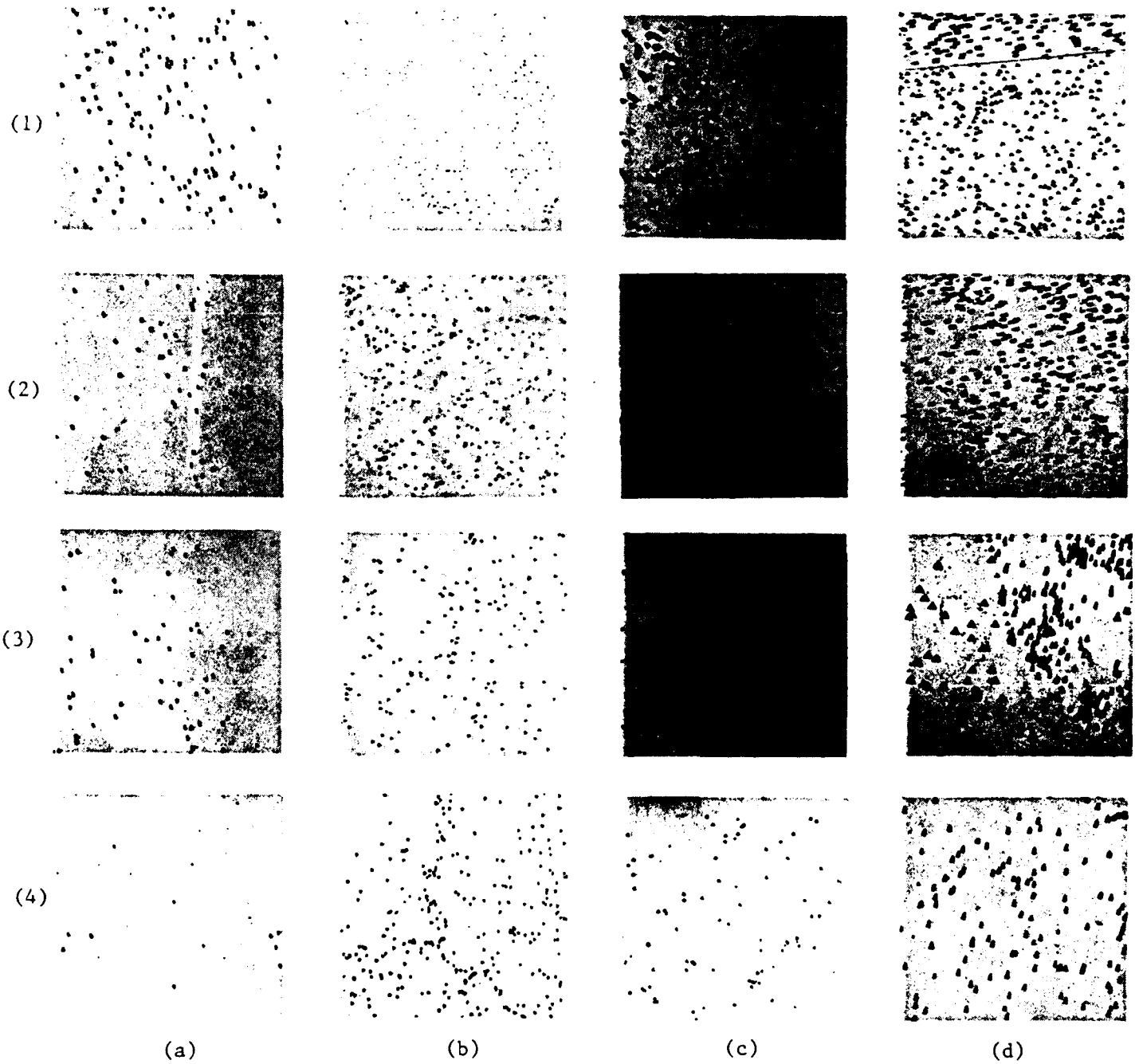

Fig. 16. Chemical etch pit studies on unoriented (a) Stanford and (b-d) commercial CdTe specimens using EAg-1 etch following chem-mechanical and chemical polishing. Etch pit densities near the centers of the respective wafers were (a) Stanford material $10-10^2$ cm^{-2}, (b) manufacturer A, $3x10^4$ cm^{-2}, (c) manufacturer B, $3x10^4$ cm^{-2} and (d) manufacturer C, $3x10^4$ cm^{-2}. Scale 100X.

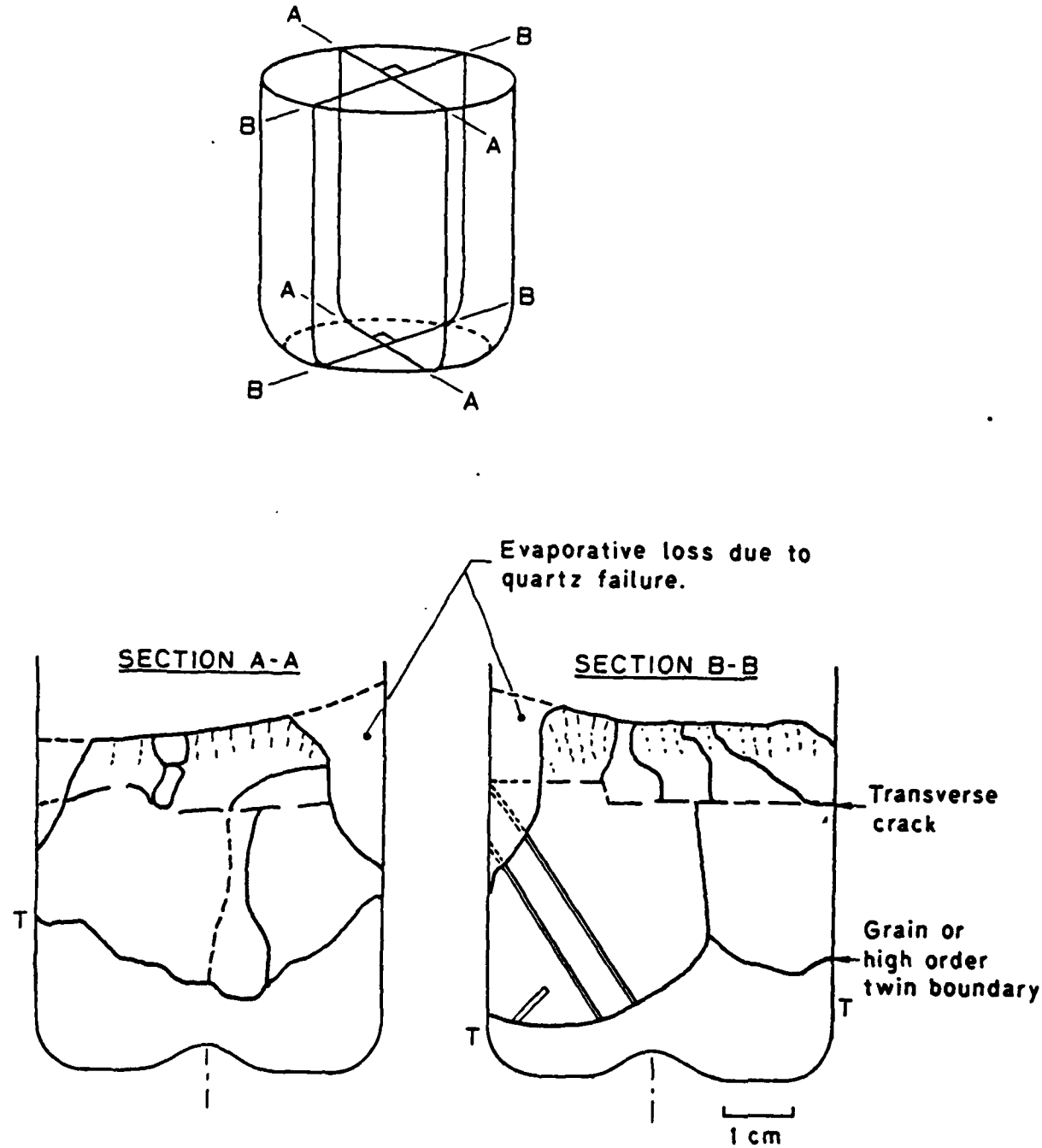

Fig. 15. Analysis of grain structure in preliminary HEM growth experiment from longitudinal sections. Initial grain selectivity was very good, and only a minor amount of lamellar twinning was seen.

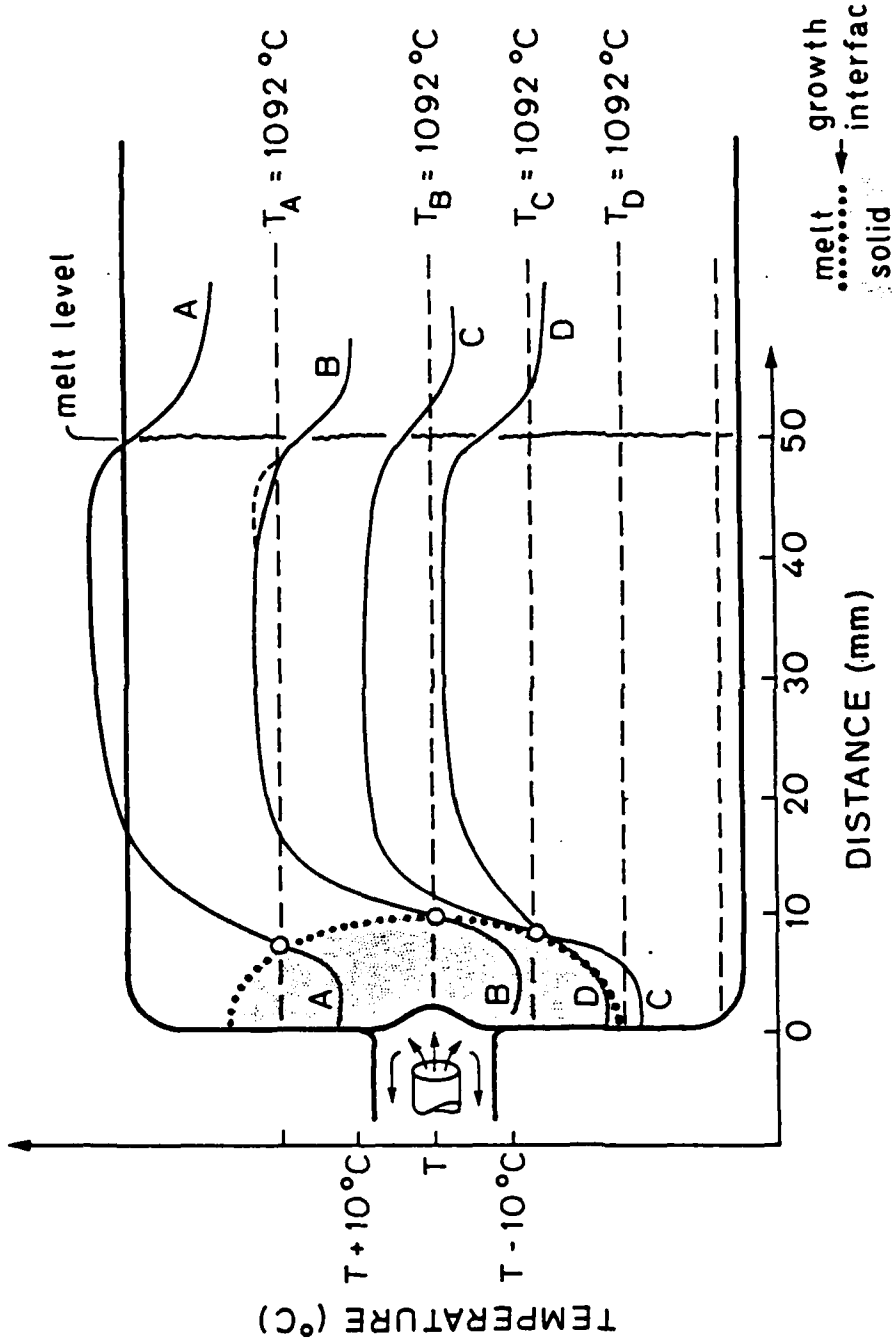

Fig. 14. Thermal analysis of the HEM melt profiling experiment. The composite of four thermal profiles A-D shows the position of the melt/solid interface along the four broken lines T_A - T_D which represent four thermocouple positions. A convex interface shape is revealed.

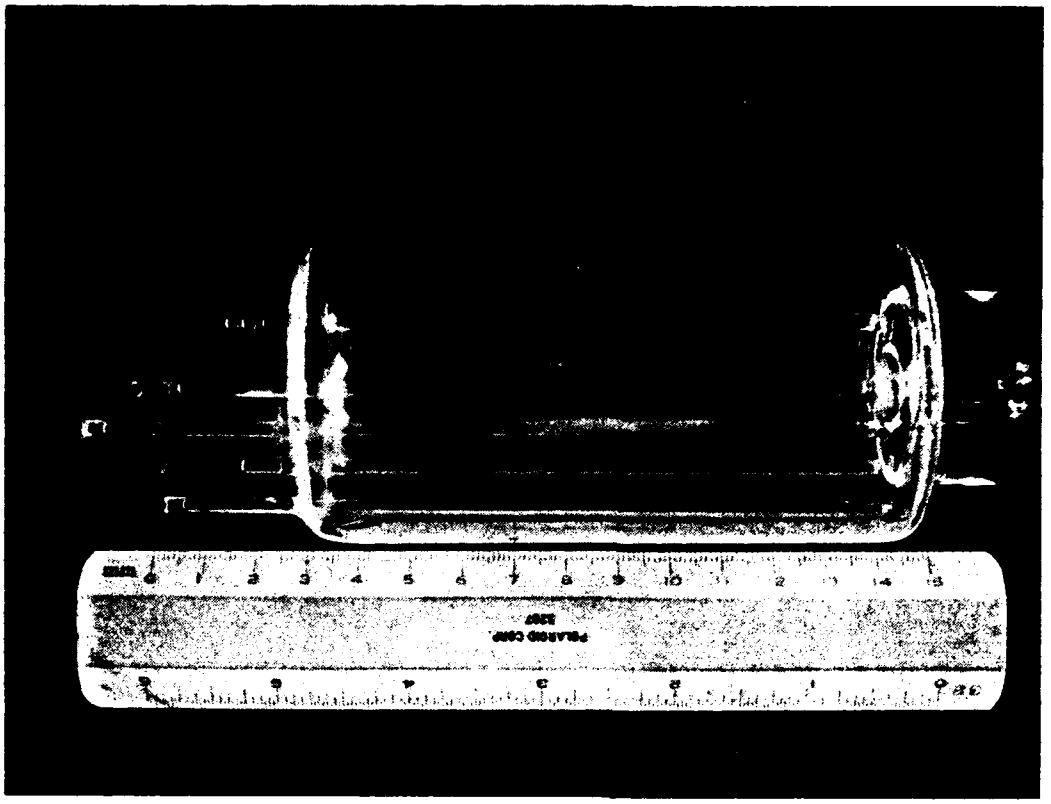

(b)

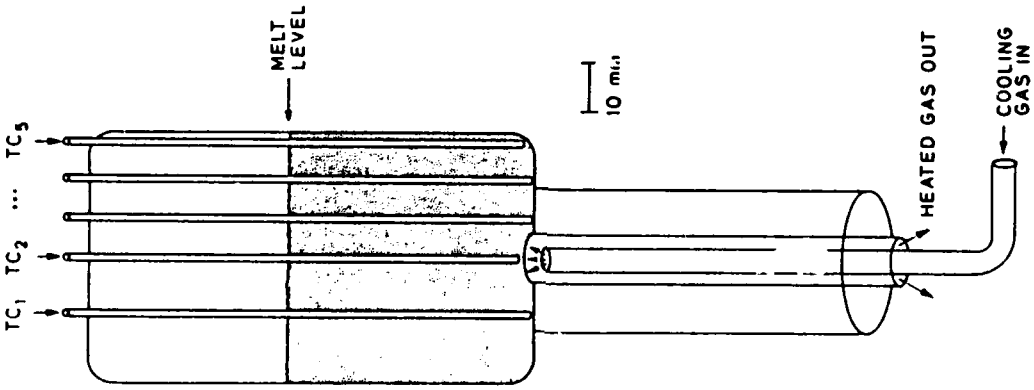

(a)

Fig. 13. Fused quartz HEM growth ampoule with five reentrant thermocouple wells. (a) Schematic and (b) photograph. The growth ampoule was 50 mm ID.

MODIFIED INTERFACE SHAPE USING THE HEAT EXCHANGER METHOD

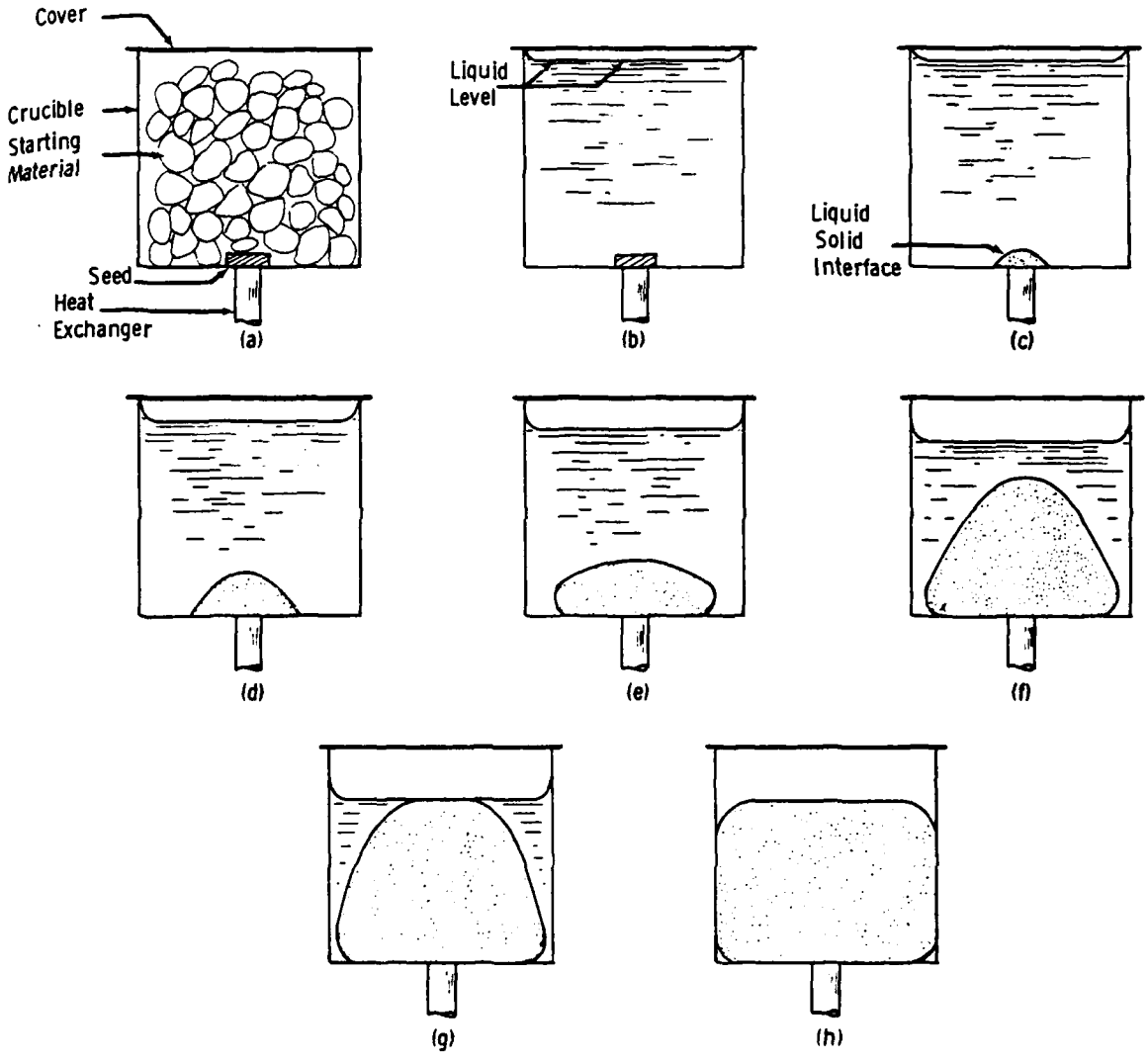

Fig. 12. Growth interface shape control using the heat exchanger method after Viechnicki and Schmid [12].

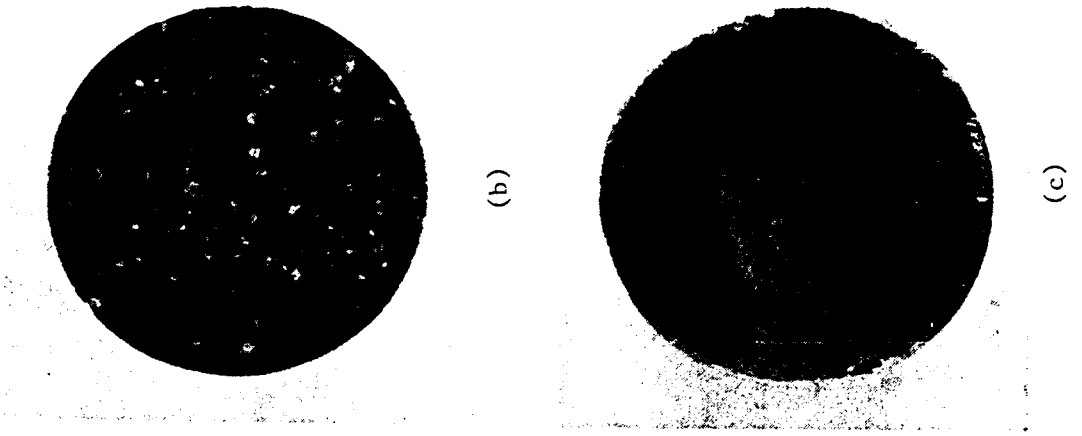

(b) (c)

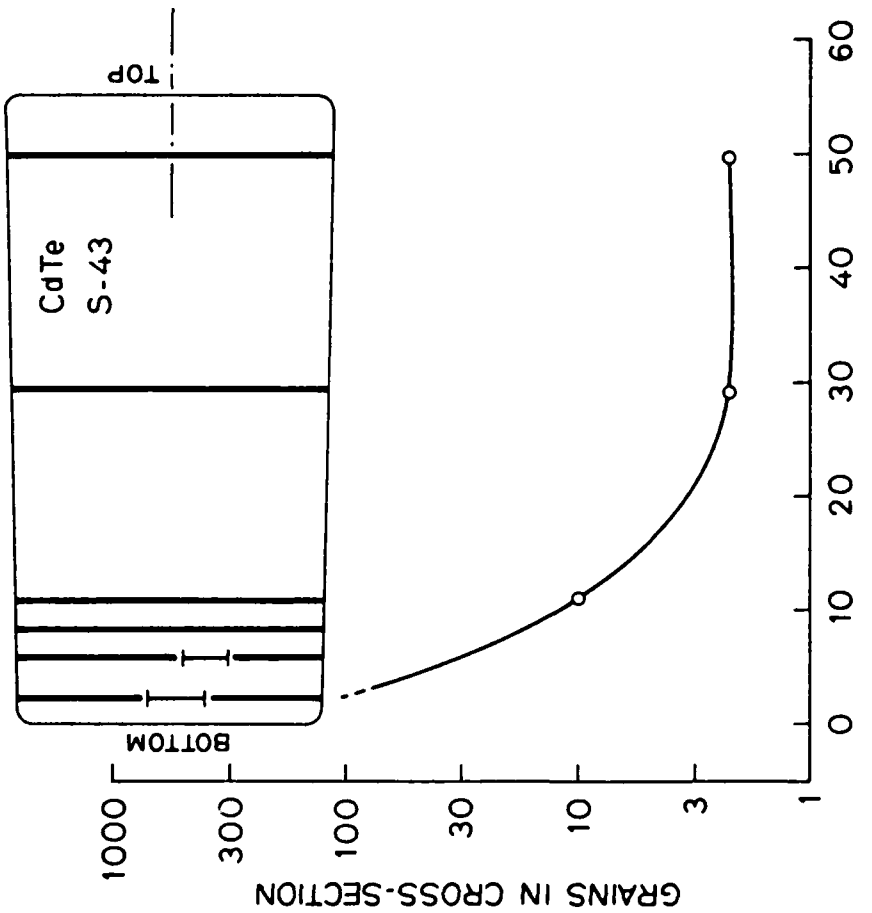

(a)

Fig. 11. Grain structure in a 30 mm dia. CdTe boule grown in a flat-bottomed growth ampoule (a). Cross-sections near the bottom (b) and near the center (c) illustrate the strong grain selectivity during the initial 3 cm. of growth.

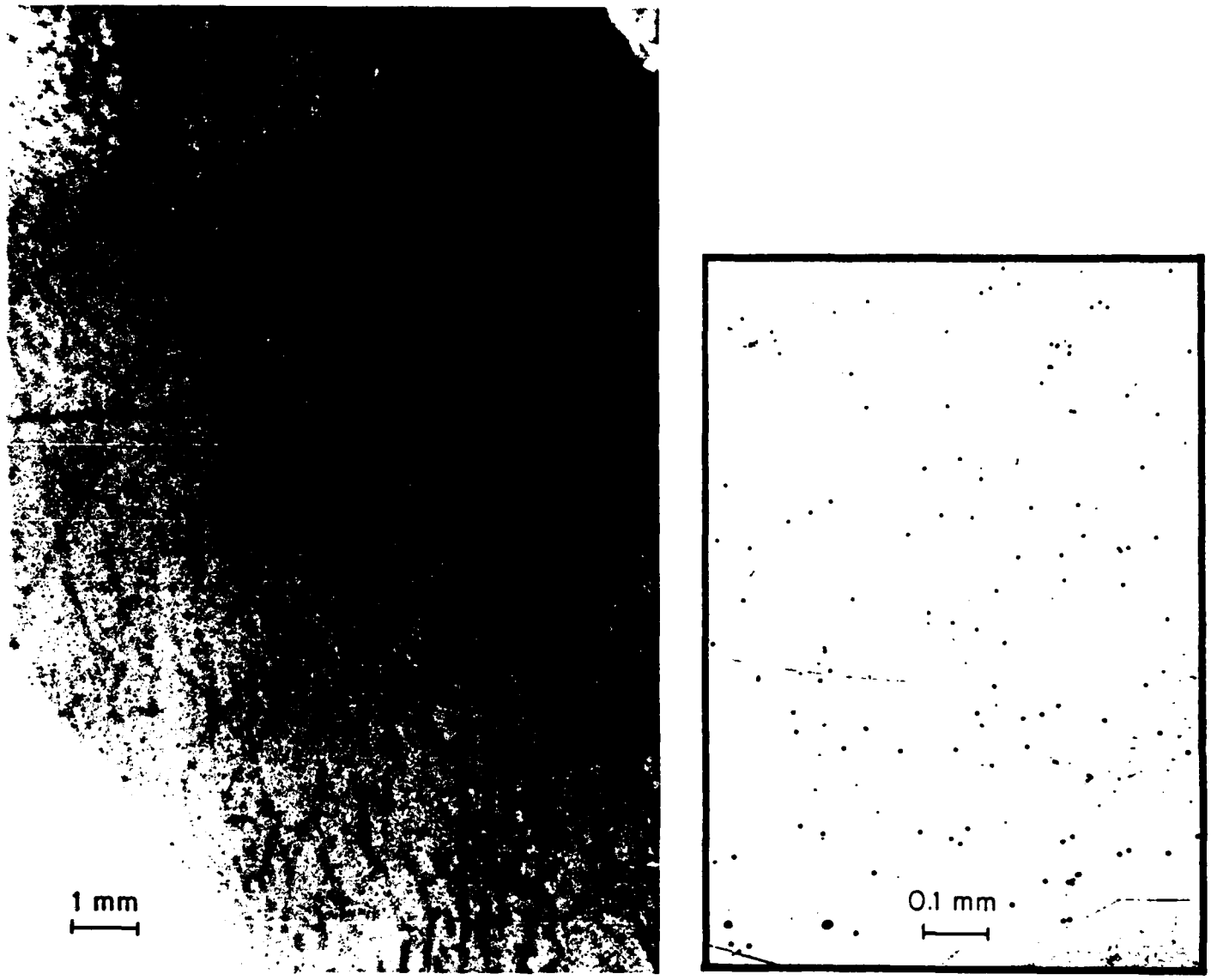

(a) (b)

Fig. 23. (a) Reflection topograph of an In-doped ($10^{19}cm^{-3}$) CdTe boule showing minimal subgrain structure. (b) Corresponding etch pit study reveals EPD $\simeq$ $10^{4}cm^{-2}$ which is in the low-defect range. The mechanism is thought to be related to solution hardening.

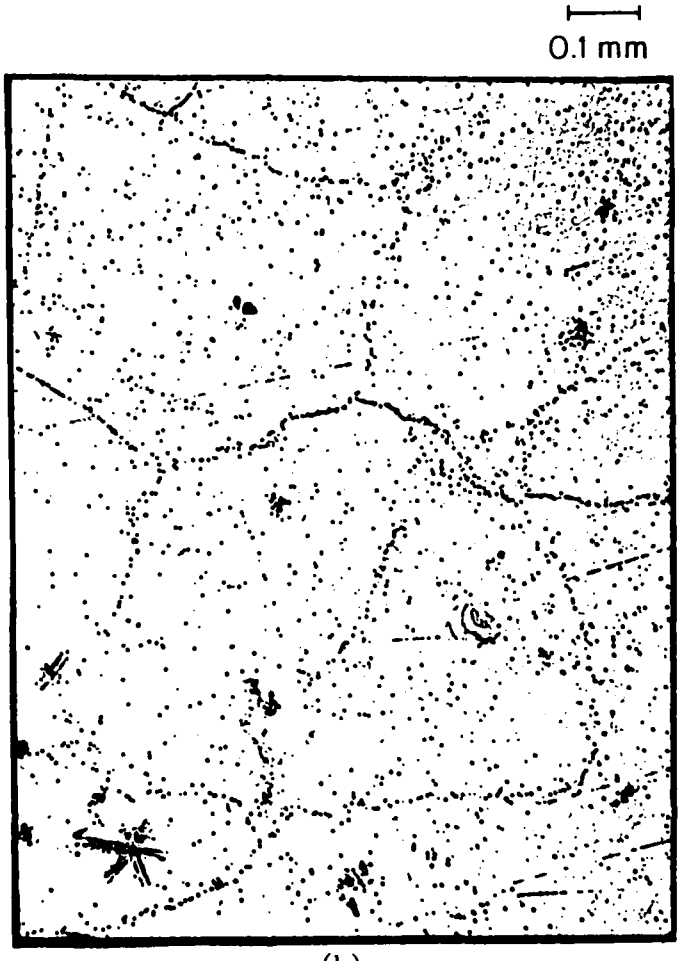

Fig. 24. Dark contrast structure in reflection topograph of commercial material (a) is strongly suggestive of subgrain boundaries revealed by chemical etching (b). Topography is sensitive to lattice distortion as well as dislocation, and some of the dark contrast features may not be revealed as dislocation etch pits, and conversely some of the dislocation structure may not appear as contrast features in topography. [0.1 mm scale]

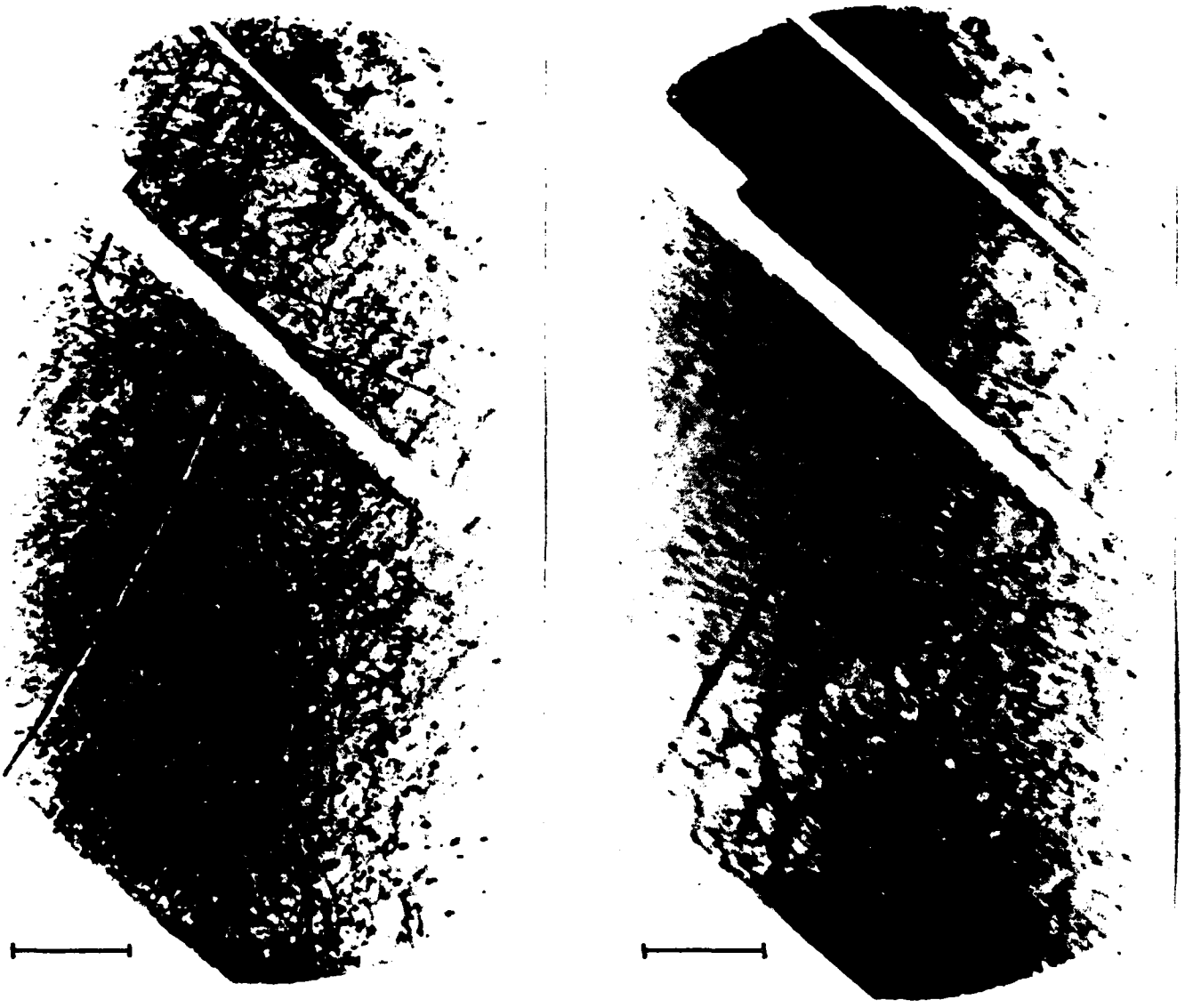

(a) (b)

Fig. 25. Transmission topographic images of a thinned CdTe specimen which shows clear features suggestive of individual dislocations within the subgrains. By using the invisibility criterion and by knowing the $\vec{g}$ vector associated with each diffraction image, one can determine the Burgers vector of selected dislocations. [Millimeter scale]

REFERENCES

1. M. Inoue, I. Teramoto, and S. Takayanagi, J. Appl. Phys. 33, 2578 (1962) and 34, 404 (1963).

2. K. Nakagawa, K. Maeda, and S. Takeuchi, Appl. Phys. Lett. 34, 574 (1979).

3. K. A. Jackson and C. E. Miller, J. Crystal Growth 42, 364 (1977).

4. A. M. Papen, M. Pettit, G. Silvestre and J. J. Bacmann, "Grain Boundaries in Semiconductors," (ed. G. E. Pike, C. H. Seager, and H. J. Leamy) Elsevier, NY (1982).

5. E. Mooser and W. B. Pearson, J. Electronics 1, 629 (1956).

6. W. A. Tiller, "The Art and Science of Growing Crystals," ed. J. J. Gilman (Wiley, New York, 1963) pp. 276-312.

7. C. E. Chang and W. R. Wilcox, J. Crystal Growth 21, 135 (1974).

8. R. S. Feigelson and R. K. Route, J. Crystal Growth 49, 261 (1980).

9. H. Kuwamoto, J. Crystal Growth 69, 204 (1984).

10. N. R. Kyle, J. Electrochem. Soc. 118, 1790 (1971).

11. T. Jasinski, W. M. Roshenow, and A. F. Witt, J. Crystal Growth 61 339 (1983).

12. D. Viechnicki and F. Schmid, J. Crystal Growth 26, 162 (1974).

13. S. L. Bell and S. Sen, in Extended Abstracts U.S. Workshop on the Physics and Chemistry of Mercury Cadmium Telluride (1984).

14. A. K. Chin, J. Electrochem. Soc. 129, 369 (1982).

15. L. O. Bubulac, W. E. Tennant, D. D. Edwall, E. R. Gertner, and J. C. Robinson, J. Vac. Sci. Technol. A3, 163 (1985).

16. B. K. Tanner, "X-Ray Diffraction Topography," Pergamon Press, Oxford (1976).

17. H. Cichey, W. Eigermann, G. Müller-Vogt, B. Schmidt and Schönholz, Hamburger Synchrotronstrahlung-slaber, HASYLAB am Deutschen Elektronen-Synchrotron DESY Jahresbericht 1983, p. 114.

18. A. W. Vere, S. Cole, and D. J. Williams, J. Electron. Materials 12, 551 (1983).

19. S. L. Bell and S. Sen, J. Vac. Sci. Technol. A3, 112 (1985).

20. N. C. Giles-Taylor, R. N. Bicknell, D. K. Blanks, T. H. Myers, and J. F. Sehetzina, J. Vac. Sci. Technol. A3, 76 (1985).

21. A. R. Wood, J. R. Schmit, K. H. Chung, T. J. Magee, and G. R. Woolhouse, J. Vac. Sci. Technol. A3, 93 (1985).

VI. PARTICIPATING SCIENTIFIC PERSONNEL

A. Professional Staff

R. S. Feigelson (Professor, Principal Investigator)

D. E. Elwell (Senior Research Associate)

R. K. Route (Senior Research Associate)

B. Technical Staff

M. Wolf (Senior Technician/Engineering Associate)

R. J. Raymakers (Senior Technician)

C. Graduate Students

Y.-C. Lu (Materials Science and Engineering, Ph.D. Program)

VII. APPENDICES (Technical Publications)

A. R. K. Route, M. Wolf and R. S. Feigelson, "Interface Studies during Vertical Bridgman CdTe Crystal Growth," J. Crystal Growth 20, 379 (1985).

B. Y.-C. Lu, R. K. Route, D. Elwell and R. S. Feigelson, "Etch Pit Studies in CdTe Crystals," J. Vac. Sci. Technol. A3 (a), 264 (1985).

VII. APPENDIX A

Journal of Crystal Growth 70 (1984) 379–385
North-Holland, Amsterdam

INTERFACE STUDIES DURING VERTICAL BRIDGMAN CdTe CRYSTAL GROWTH

R.K. ROUTE, M. WOLF and R.S. FEIGELSON

Center for Materials Research, Stanford University, Stanford, California 94305, USA

The purpose of this study was to reveal the shape of the melt/solid interface, and its influence on boule quality, during the vertical Bridgman melt growth of CdTe crystals. ^{111}In, with a half-life of 2.8 days, was used as a radiotracing dopant, and sharp growth rate perturbations were used to incorporate it in bands corresponding to the melt/solid interface during otherwise normal crystal growth. Autoradiography was used to reveal their actual shapes, which were found to be almost flat. Slightly convex interface shapes were generated by thermal modifications, but no significant improvements in grain structure (large grain, polycrystalline) were noted. Growth rate histograms showed that furnace end effects can be a dominant factor in Bridgman systems, and can cause significant differences between imposed and actual growth rates.

1. Introduction

Depending on its application, CdTe is grown by a variety of different growth methods. For use as IR detector substrates and electro-optic modulators, crystal growth from the melt by the Bridgman technique is preferred because of its simplicity and its relatively high growth rates compared with vapor and solution growth methods. After more than a decade of intensive research in the Bridgman melt growth of CdTe, it is still not known with certainty why the material so often grows as a large-grain polycrystal, usually with the presence of lamellar or micro-twins. Crystal growth systems today have been empirically tuned to the point where occasionally largely single crystal ingots are produced, and more often a significant fraction of an ingot will be found to be single and not heavily twinned. However, total control over boule crystallographic structure and growth direction has not yet been achieved. A substantial fraction of CdTe Bridgman melt growth today is still being carried out unseeded.

In our experiments on the growth of CdTe crystals by the vertical Bridgman method, the significant problem appeared to be a relatively poor grain selection mechanism coupled with occasional secondary nucleation. In most cases, the secondary grains appeared to nucleate at the surface of the boule where the freezing interface was in contact with the quartz growth ampoule. Secondary grains, once formed, would often grow both inward and larger. One possible explanation for such behavior was felt to be the shape of the melt/solid interface. It is commonly held that an optimum melt/solid interface shape is slightly convex with respect to the solid, a situation which should force surface-related defects to grow out [1]. Conversely, a concave interface may promote the growth inward of surface-related defects and secondary grains. These hypotheses have never been thoroughly demonstrated for compound semiconductors that must be grown in sealed quartz ampoules, however, due to the difficulties in revealing melt/solid interface shapes and with the practical difficulty of making a significant change in that interface shape.

We describe in this paper, experiments designed to reveal progressive melt/solid interface shapes during the vertical Bridgman melt growth of CdTe boules. Because of its relative ease, we chose to demark melt/solid interface shapes using a radiotracer technique like that reported by Kyle [2] in earlier experiments on CdTe. An alternative technique which gives much finer resolution is current induced interface demarcation [3]. For implementation, however, it requires two electrical feedthroughs [4] which are difficult to incorporate into sealed quartz growth ampoules like those used to grow CdTe crystals. In our experiments, the melt was doped with radioactive indium (^{111}In) having a nominal half-life of 2.8 days. The segregation coefficient of In in CdTe has

0022-0248/84/$03.00

been variously reported in the range 0.1–0.5 [5–7] over near-congruent melts depending on the Cd overpressure. Under normal growth conditions it is therefore segregated uniformly from the growing crystal. By sharply speeding up the growth rate at various times during growth, bands containing higher concentrations of ^{111}In can be frozen in at the melt. solid interface. Autoradiographic techniques can then be used to reveal the shape of the melt/solid interface corresponding to each thermal event.

2. Experimental procedure

CdTe crystals were typically grown in a conventional two-zone Bridgman furnace having a "booster heater" at the bottom end of the upper zone, fig. 1a. The furnace bore was 63 mm (2.5 inch) and a fused silica sleeve was used for partial containment in case of ampoule failure and to reduce convection. Typical temperature profiles obtained in the empty furnace are shown in fig. 1b. Long term temperature stability was in the range of ± 0.5°C and short term fluctuations were even less, within the noise of the monitoring equipment. Temperature gradients were modified during the course of the experiments and gradients in the empty furnace varied in the range from 2–20°C/cm at a nominal melting point of 1096°C. Maximum temperatures in the furnaces were limited to 1140°C in order to minimize effects due to softening of the fused quartz growth ampoules.

Growth ampoules were constructed of 2 mm wall fused quartz tubing. The main bodies were continuously tapered outward at 3/4° for 15 cm to a maximum diameter of 28 mm to prevent keying of the boules after growth. Most of the ampoules were designed to accommodate a square seed 8 mm^2 × 40 mm long, although seeds were not used in these experiments. In a few experiments, however, ampoules having slightly longer cylindrical seed pockets were used. As is typical, the inside surfaces of the ampoules were coated with an opaque layer of

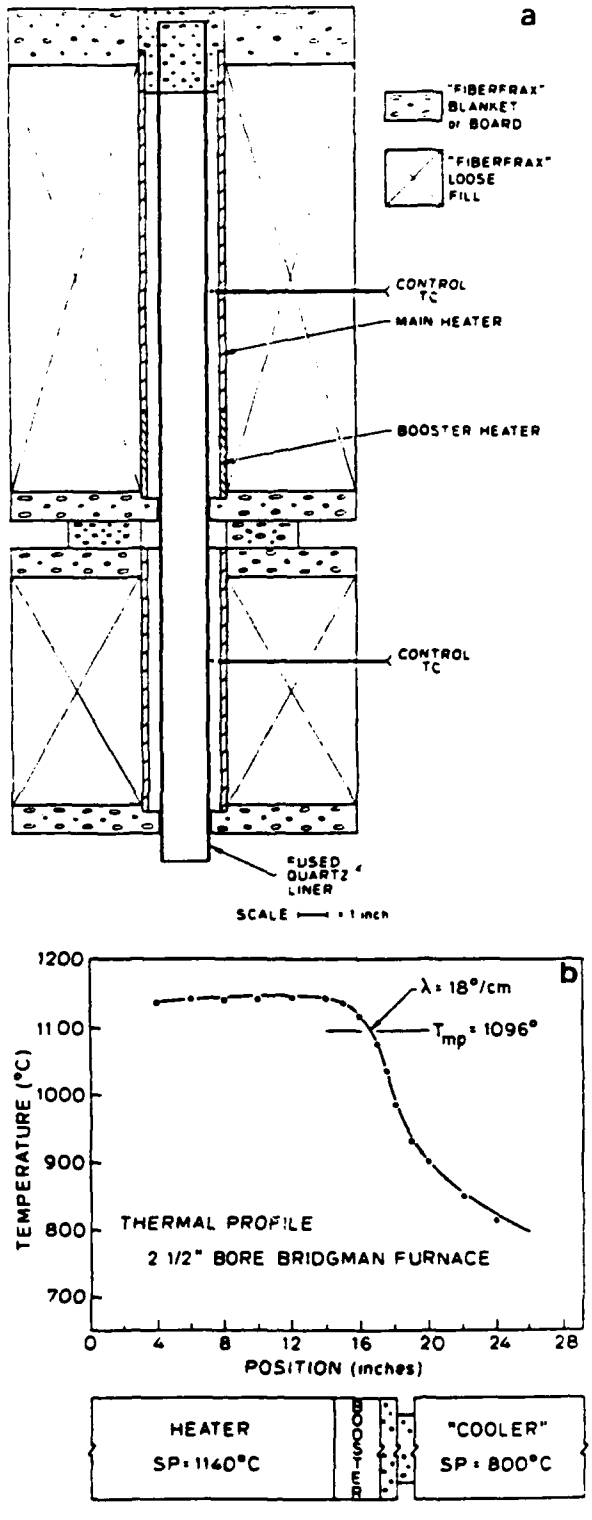

Fig. 1. (a) Details of vertical Bridgman furnace construction. The ratio of booster power to main heater power was fixed by a "Variac" divider and determined experimentally by optimizing the thermal profile in the furnaces. (b) Typical temperature profile obtained in an empty furnace.

carbon by the pyrolysis at 1000°C of hexane carried on an argon stream. Charges were all sealed into the quartz ampoules under a vacuum of 10^{-5} Torr or better. Platinum–rhodium reference thermocouples were then fixed to the outsides of the fused quartz growth ampoules at a position approximately 1.5 cm from the bottom of the seed pocket.

CdTe charges for these experiments, weighing typically 150–200 g, were either synthesized in our laboratory from nominal 5-9's high purity elements, or were obtained in the form of polycrystalline ingots of 5-9's or better purity, all of which came from Cominco, Inc.

The radiotracer used was ^{111}In obtained from New England Nuclear in 0.05 M HCl solution. Activities of approximately 150 μCi were pipetted directly into the quartz growth ampoules and taken to dryness over aperiod of 2 h in a 90°C oven. Additional metallic indium was added to the crushed CdTe charge in order to bring the overall doping level into the 10^{18}–10^{19} cm^{-3} range. The charges were then vacuum sealed in the quartz growth ampoules.

The interface demarcation technique was superimposed on otherwise regular CdTe crystal growth procedures. In our experimental setup, the ampoules are held from the bottom by a rigid quartz rod, and the furnaces are slowly raised on a mechanical frame in order to effect unidirectional solidification. The furnace translation rate in all experiments was 1.1 ± 0.1 mm/h. It was experimentally determined that a relatively sharp increase in growth rate was required to incorporate sufficient ^{111}In for effective interface demarcation. To accomplish this, power to the growth furnace was interrupted for one minute and at the end of this period the furnace was translated manually by 2 mm in the growth direction. Power and the standard growth translation rate were then restored. Temperature excursions at the position of the control thermocouple were -20°C to -30°C and recovery occurred after approximately 15 min. Demarcation events carried out at $1\frac{1}{2}$ h intervals (1.5 mm spacing) were resolvable, although normally they were spaced by approximately 12 h. Coding sequences were used to unambiguously relate the incorporated bands to the demarcation sequence.

At the termination of growth, the boules were cooled at ~100°C/h, removed, partially encapsulated in plaster of paris, and split axially with a diamond saw. After a light abrasive cleaning to remove accumulated fine particles left from sawing, the boule sections were placed in direct contact with double emulsion Kodak no-screen X-ray film, S0-445, and left for exposure for periods varying from several hours to nine days. Total remaining activity at the beginning of exposure was estimated to be in the 25–40 μCi range, most of which was located at the very top of the boules as one would expect from normal segregation. Exposure periods of several days were required to adequately reveal the significantly smaller amounts incorporated in bands along the lengths of the boules.

3. Results of interface shape studies

A longitudinal section through a CdTe boule grown under nominal growth conditions is shown in fig. 2a, where much of the macroscopic structure such as grain boundaries and twins typically seen in CdTe is revealed. In fig. 2b, we show the corresponding contact autoradiograph. Fully exposed radiographs revealed a series of faint somewhat

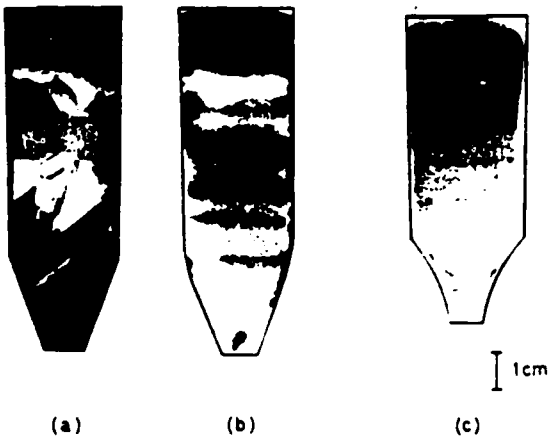

Fig. 2. (a) Longitudinal section of a CdTe boule grown under nominal growth conditions. Twin boundaries, lamellar twins, and non-planar incoherent grain boundaries can be seen. (b) Radiograph obtained by 4-day contact exposure with boule section containing ~20 μCi activity at the beginning of exposure. The large accumulation of ^{111}In at the top of the boule reflects normal segregation behavior. (c) Interface bands observed in a high gradient case with an air-cooled seed from an experiment to generate convex melt/solid interface shapes.

diffuse bands approximately 1–2 mm wide distributed along the lengths of the boules. The diffuse bands were uniform in density across the boule sections and correspond in width to the 2 mm mechanical perturbations introduced during each demarcation event. Parallel experiments carried out with power interruption alone produced no discernable bands, suggesting that remelting rates during recovery were rapid compared to the normal growth rate. It therefore may be assumed that the diffuse bands accurately reflect the shape of the steady-state growth interface at the time of each demarcation event. The results suggested relatively flat interface shapes throughout the entire growth sequence, a finding in basic agreement with that reported earlier by Kyle [2].

Experiments were next carried out to modify the shape of the melt/solid interfaces by changing the furnace temperature gradient and to ascertain whether significant changes in crystallographic grain structure would result. The one-dimensional theory of Chang and Wilcox [8] suggests that by steepening the temperature gradients below the melting point which ideally should be located at the knee of the furnace temperature profile, the melting point isotherm can be raised slightly in the furnace and a more convex interface shape should be obtained. (This conclusion was demonstrated earlier by the authors for the case of $CdGeAs_2$ [9] which melts at a significantly lower temperature, $T_{mp} = 659^\circ C$.) The growth furnace was modified to increase booster power capability and air-cooling at the bottom of the seed pocket was introduced to increase heat extraction from the bottom end of the boule. Temperature profiles in the empty furnace became meaningless with air cooling present. However, $(\Delta T/\Delta z)_{1096^\circ C}$ obtained during the growth experiment from the reference thermocouples was considered to reflect the changes in thermal gradients that we were able to achieve. In our usual growth experiments $(\Delta T/\Delta z)_{1096^\circ C} = 1^\circ C/mm$, while in the enhanced gradient case $(\Delta T/\Delta z)_{1096^\circ C} = 1.7^\circ C/mm$. Interface shapes in the latter case were only slightly more convex than in the normal gradient, fig. 2c, and the grain structure of the boules was not significantly improved. In axial sections, all of the boules in this study contained 6–20 grains. An accurate comparison of boule structure was impossible because of the statistical fluctuations that always occur from one boule to another. While our assessment of boule grain structure was, therefore, subjective, it did include the experience gained from the growth of a large number of CdTe boules in associated programs.

The converse situation in which a crystal was grown in a uniform, shallow gradient, $(\Delta T/\Delta z)_{1096^\circ C} = 0.2^\circ C/cm$, did not produce concave interface shapes as might be expected from a typical semiconductor where the melt has higher thermal conductivity than the solid. Interface shapes were again found to be almost flat and no significant differences in grain structure were noted in the grown boules.

4. Discussion

The experiments to modify the steady-state growth interface shapes using heat flow considerations from the one-dimensional theory of Chang and Wilcox [8] were only marginally successful. In the enhanced gradient experiments designed to make more convex interface shapes, the axial gradients achieved were not particularly large compared to typical high gradient values in the 100°C/cm range. Furnace bore has some influence, however, and one usually anticipates lower axial temperature gradients as furnace bores increase. (The furnace bore in our experiments was 62.5 mm.) The need to limit maximum furnace temperatures to $T \leq 1140^\circ C$ to prevent softening and possible swelling of the growth ampoule was a more significant limitation and prevented us from operating on the steeper section of the furnace temperature profile.

In the shallow gradient experiments, the one-dimensional theory of heat flow [8] predicts concave interface shapes for typical semiconductors where the thermal conductivity of the liquid is assumed to be greater than that of the solid. The flat growth interfaces actually found could be caused by two factors. First, because of its low thermal conductivity, we expect CdTe to have relatively high effective Biot numbers [10] and therefore expect only moderate interface curvatures at best [8]. Second, flat interface shapes could indicate that the thermal conductivity of liquid CdTe may be much closer to

that of the solid than is typical for semiconductors. Ionic materials often exhibit a lower thermal conductivity in the liquid phase and, due to its high ionicity (0.7 on the Phillips scale), it may not be surprising for CdTe to behave like an ionic material in this respect.

Our initial conclusions from this study are that (1) in typical CdTe vertical Bridgman growth systems generally flat melt/solid interface shapes seem to be the norm in the regime where growth rates are not so high that the latent heat of fusion becomes a significant factor; (2) it is possible within the constraints of furnace construction and maximum operating temperature to produce slightly convex (favorable) melt/solid interface shapes, but major changes in interface shape are very difficult to achieve; (3) no major improvement in grain structure results from making minor changes to otherwise flat interfaces; and (4) the difference between melt and solid thermal conductivity may not be as great as those observed in less ionic semiconductor systems.

Several other observations can also be made from these experiments. The location of the melt/solid interface bands provides an accurate growth rate histogram for each boule. In several of our experiments, the initial demarcation event was introduced when the reference thermocouple was near T_{mp} = 1096 °C. The first interface band was found reasonably close to this position. In fig. 3a we compare the positions where interface demarcation events were introduced with those actually found, and a considerable discrepancy is seen. In fig. 3b we plot the two positions. It can be seen that although the growth rate of the crystal matches the rate of travel of the furnace within the 4 cm long seed pocket, once the interface reaches the main body of the growth ampoule, the growth rate begins to lag the furnace travel rate. It appears to reach a relatively uniform value which, taking into account the 2 mm jogs at each demarcation event, was calculated to be 35% lower than the furnace translation rate. Similar behavior was noted in all three thermal gradient conditions studied. This obviously cannot represent a true steady-state situation in a semi-infinite growth ampoule, where after some readjustment of interface position, the two rates would again have to agree. But in a practical Bridgman crystal growth situation where the boule is only a few ampoule diameters in length we find a very significant reduction in actual growth rate throughout the entire main body of the crystal. Because of the low furnace travel rate in these experiments, 1 mm/h, we assume that the

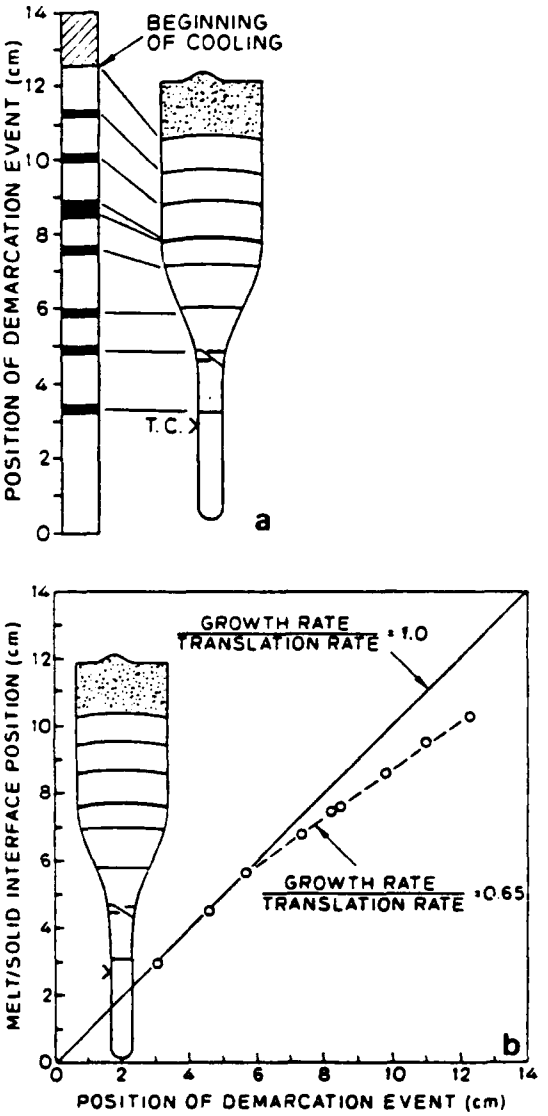

Fig. 3. (a) Comparison between relative position of interface demarcation events vs. the corresponding interface positions actually observed. The progressive lag throughout the main body of the boule indicates a reduced growth rate. Premature cooling is also observed. (b) Plot of demarcation event position versus melt/solid interface position. Relatively uniform, but reduced growth rate is seen throughout the main body of the boule. The reduction is growth rate in this case was 35%.

latent heat of solidification contributes negligibly to this effect and that it is due primarily to furnace end effects. In a more comprehensive study of this phenomenon, Wang, Witt, and Carruthers [11] have found similar end effects in the Ga-doped Ge system using current-induced interface demarcation in a single zone vertical Bridgman growth system. Until we became aware of the magnitude of this effect in the CdTe system, several of the interface demarcation experiments were terminated before the boules had completely solidified, leaving a region of more rapidly solidified material containing significantly higher levels of ^{111}In and presumably other impurities as well at the tops of the boules, as shown in fig. 3a. (Because CdTe can tolerate relatively rapid growth rates, premature cooling does not reveal itself by an immediate change in grain structure or interface breakdown, and therefore we conclude that rapid cooling alone is not an effective technique for revealing the interface shape in CdTe.)

The existance of furnace end effects is well known, but their magnitude in practical growth systems may not always be appreciated. End effects can be influenced by a number of factors including placement of the control thermocouple, which in these experiments was relatively high in the upper zone, and by changes in the thermal coupling factors between the various sections of the furnace due to motion of the boule during growth. In our particular case, by lowering the boule toward the insulating region between the upper and lower furnaces, radiative heat losses from the upper furnace appeared to be reduced. This allowed the lower end of the upper furnace to become hotter and forced the melting point isotherm in the growth ampoule to a lower position. The net result was the very significant reduction in growth rate observed, and a lowering of interface location by an amount approaching one full boule diameter. From the one and two dimensional numerical models in the literature, one expects exactly the opposite behavior, where an increase in growth rate is usually predicted (refs. [10, 12–14] as examples).

We conclude that "configurational" end effects can play a significant role in practical Bridgman melt growth systems. The control of melt/solid interface shape by manipulation of the relative heat flux in the system [8,9] could be greatly complicated by this phenomenon. Comparison with experiment in practical semiconductor systems, should therefore be carried out with appropriate attention to careful thermal monitoring.

5. Summary

We have used ^{111}In as a radiotracing dopant for melt/solid interface shape demarcation during vertical Bridgman melt growth of CdTe. Relatively low activities of this short half-lived isotope were shown to reveal well-defined interface shapes. The interface shapes were found to be near-optimal and varied from marginally concave to slightly convex. Attempts to modify them were successful but produced only slight changes. Furthermore, no significant differences in boule grain structure were noted. Growth with a continuously convex interface shape produced no apparent improvement over control boules grown under essentially flat interface conditions.

Furthermore, a series of interface demarcation events was found to reveal useful information in the form of a growth histogram of each boule. From this data, furnace end effects were found to be a significant factor in the typical Bridgman growth system used for these experiments. Crystal growth rates were as much as 35% lower than the imposed mechanical translation rate throughout the main body of the boule, and melt/solid interface positions were found to move correspondingly lower in the furnace as growth proceeded. This phenomenon suggests complex boundary conditions that complicate comparison with the theoretical modelling studies of Bridgman growth systems.

Acknowledgement

This work was supported in part by the Army Research Office through grant DAAG29-83-K-0023, and in part by the NSF-MRL Program through the Center for Materials Research, Stanford University.

References

[1] W.A. Tiller, Principles of Solidification, in: The Art and Science of Growing Crystals, Ed. J.J. Gilman (Wiley, New York, 1963) pp. 276–312.

[2] N.R. Kyle, J. Electrochem. Soc. 118 (1971) 1790.

[3] R. Singh, A.F. Witt and H.C. Gatos, J. Electrochem. Soc. 115 (1968) 112.

[4] R.K. Crouch, W.J. Debnam and R. Ryan, J. Crystal Growth 56 (1982) 215.

[5] M. Yokozawa, S. Otsuka and S. Takayanagi, Japan. J. Appl. Phys. 4 (1965) 1018.

[6] K. Mizuma, O. Mikami, K. Ono and Y. Kamiya, Elec. Commun. Lab. Tech. J. 10 (1961) 895.

[7] L. Thomassen, D.R. Mason, G.D. Rose, J.C. Sarace and G.A. Schmitt, J. Electrochem. Soc. 110 (1963) 1127.

[8] C.E. Chang and W.R. Wilcox, J. Crystal Growth 21 (1974) 135.

[9] R.S. Feigelson and R.K. Route, J. Crystal Growth 49 (1980) 261.

[10] T. Jasinski, W.M. Rohsenow and A.F. Witt, J. Crystal Growth 61 (1983) 339.

[11] C.A. Wang, A.F. Witt and J.R. Carruthers, Analysis of Crystal Growth Characteristics in a Conventional Vertical Bridgman Configuration, preprint courtesy of authors.

[12] J.P. Riquet and F. Durand, J. Crystal Growth 33 (1976) 303.

[13] T.W. Clyne, J. Crystal Growth 50 (1980) 684.

[14] P.C. Sukanek, J. Crystal Growth 58 (1982) 208.

VII. APPENDIX B

Etch pit studies in CdTe crystals

Y.-C. Lu, R. K. Route, D. Elwell, and R. S. Feigelson
Center for Materials Research, Stanford University, Stanford, California 94305

(Received 15 June 1984; accepted 5 October 1984)

Etch pit formation has been studied on (111)A, (111)B, and (100)CdTe surfaces using a nitric acid/potassium bichromate etch with varying Ag^+ ion concentrations. The results can best be explained using an adsorption poisoning model originally proposed to explain etch pit formation in InSb, with modifications to take into account the higher ionicity of CdTe. Although the results were fairly reproducible, the etch pit density was consistently lower than that obtained with the Nakagawa etch. $A\beta$ dislocation pits were seen for the first time in CdTe.

I. INTRODUCTION

Cadmium telluride has important applications as an oriented {111} substrate for HgCdTe epitaxial infrared detectors. Because defects such as dislocations can propagate from the substrate and degrade epitaxial device performance, the determination and control of defect density in bulk CdTe substrate material is of great importance. Chemical etching methods have been the mainstay for the determination of dislocation densities for a number of years, although recently a more powerful and diverse group of techniques has begun to be utilized. This study was an in-depth investigation of the etching behavior of CdTe using established etches, the eventual aim being the development of a simple technique for defect characterization.

CdTe has the zinc-blende structure, which belongs to the space group $F\bar{4}3m$. There are two types of {111} surfaces in the CdTe structure, one composed of Cd atoms designated as (111)A, and the other composed of Te atoms designated as (111)B. Along the ⟨111⟩ direction, these planes are arranged sequentially with different and alternate interplanar spacings. The ⟨111⟩ direction is known as the polar axis, and the physical and chemical properties are quite different in opposite directions.

There are also two different kinds of edge dislocations in the CdTe structure. One is terminated in a row of Cd atoms (α dislocations); the other terminates in a row of Te atoms (β dislocations). In pure form both travel along ⟨110⟩ crystallographic directions. Four combinations between edge dislocations and {111} planes exist, namely, $A\alpha$, $B\alpha$, $A\beta$, and $B\beta$. One might expect, therefore, to find as many as four characteristically different etch pits on the polar surfaces, and perhaps two on the nonpolar surfaces.

The etching behavior on polar {111} and nonpolar {100} CdTe surfaces has been studied by a number of authors[1–6] using a variety of etches. Two of the most common etching solutions were used in this study. One is the EAg solution developed by Inoue *et al.*,[1,2] and the other, developed by Nakagawa *et al.*,[3] we refer to as the "*N*" solution.

The bulk of our etching studies were carried out with the EAg solutions since they produce etch pit figures that vary in shape depending on both the surface orientation being studied and the Ag^+ ion concentration. They are not commonly used for accurate determination of etch pit densities, however, although a systematic evaluation of their possible use for quantitative studies does not appear to have been reported. These etches are thought to reveal both types of edge dislocations depending on the Ag^+ concentration. In our studies, parallel experiments using the *N* solutions were carried out for comparison.

To account for the bulk of our results obtained with EAg solutions, we rely on a theory of adsorption poisoning which takes into account the relative reactivity of the polar surfaces and the relatively high ionicity of CdTe compared to other compound semiconductors. This type of theory has previously been applied only to III–V materials.

II. EXPERIMENTAL PROCEDURE

Oriented samples of CdTe approximately 5 mm thick were cut from crystals grown in this laboratory by the vertical Bridgman method. The crystals selected were essentially single, with some small surface grains, and twins. The crystals were oriented by Laue x-ray diffraction and cut with an abrasive wire saw along {111} and {100} surfaces. Many of the samples did contain the usual lamellar twins, and these were found to be useful in determining crystallographic directions on the {111} surfaces. Twins in CdTe are of the 180° rotation type, so that on a {111} surface containing lamellar twins, the twinned regions are relatively close to a true {100} surface, being tipped 16.8° about a ⟨110⟩ zone. Etch pits formed in these twinned regions are quite similar to those formed on true {100} planes and some of the photomicrographs shown here include twinned regions. The specimens were chemomechanically polished using a Geoscience "Politex Supreme" pad, and either a 1.5 vol % Br ethylene glycol or a 1.5 vol % Br propylene glycol solution. The high molecular weight glycols, being quite viscous compared to methanol, allow only minimal contact between the polishing pad and the workpiece, and flat, shiny surfaces, free of scratches under microscopic examination, were readily produced. The total amount of material removed by chemomechanical polishing was on the order of 250–750 μm, far more than necessary to remove work damage due to sawing. The absolute polarity assignments of the {111} samples were made following the etching behavior reported by Inoue.[1,2]

For most of our etching experiments, the specimens were polished on both surfaces and were then chemically polished with E solution for 30 s to 1.5 min prior to being selectively etched. Compositions of all the chemical etches used are shown in Table I. After chemical polishing, the samples were etched with fresh EAg 1 or EAg 2 for 20 to 60 s, under both

TABLE I. Chemical composition of polishing and etching solutions.

Symbol	Composition		Action
E (Ref. 1)	HNO_3	10 ml	
	H_2O	20 ml	polishing
	$K_2Cr_2O_7$	4 g	
EAg 1 (Ref. 1)	E solution	10 ml	
	$AgNO_3$	0.5 mg	etching
EAg 2 (Ref. 1)	E solution	10 ml	etching
	$AgNO_3$	10 mg	
N (Ref. 3)	H_2O	20 ml	etching
	H_2O_2	20 ml	
	HF	30 ml	

quiescent and agitated conditions. Agitation was by gas bubbler, teflon paddle, or by hand, and ranged from gentle to violent stirring. In parallel studies with the *N* solution, we first chemically polished with E solution for 1 min, then etched with the *N* solution for 20 to 60 s. This was immediately followed by a one-second dip in E solution to remove the dark stain that usually occurs when using *N* solution. All of the etching procedures were carried out at 23 °C, and in many cases both surfaces were etched at the same time to compare the size and morphology of the etch pits on opposite surfaces.

In certain instances, repeat etching or repeat polishing and etching were carried out to study the repeatability of the etching procedures. In these experiments the oriented samples remained on the nonreactive glass polishing fixture and only one side of each sample was etched. However, numerous samples were mounted on the fixture at one time, permitting the simultaneous study of both A and B surfaces. For the repeat polishing and etching experiments, the previous etching features were removed by chemomechanical polishing only. Total material removal in these cases was significantly less, on the order of 25 μm, which was determined by the known etching rates and the times required to eliminate the previous set of etch pits. Analysis of etch pit morphology and etch pit density was carried out using optical microscopy and scanning electron microscopy.

III. RESULTS

All orientations of CdTe surfaces, including randomly oriented grains on the edges of a number of samples, were found to form etch pits in EAg solutions. This was in contrast to the *N* solution which forms etch pits only on one CdTe(111) surface. The definition and morphology of the etch pit figures formed in EAg solutions was found to depend strongly on the Ag^+ concentration and agitation conditions. Those formed in *N* solutions were always shallow and roughly spherical in shape. In Fig. 1, a graphical representation is given of the etch pit morphologies observed, as a function of substrate orientation and etching conditions. Also shown are the relative size differences that were observed on etching both surfaces of the test samples at the same time. Noticeable size differences were, as expected, found only on the polar {111} surfaces. The graphical figures are somewhat idealized; in most cases the etch pits were not so perfectly formed. It was normally possible to determine from optical microscopy whether a set of characteristic etch pits was pyramidal or flat bottomed. However, SEM with its much greater depth of field and resolving power, was relied upon to provide additional details about the interior surfaces of the etch pits. Figure 2 shows photomicrographs of the four types of etch pits observed with EAg solutions, and Fig. 3 shows the type of etch pits typically seen with *N* solutions.

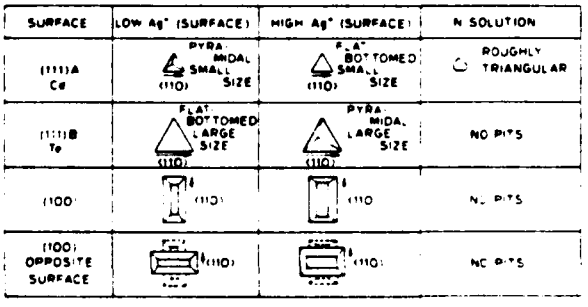

FIG. 1. Typical etch pit morphologies on (111) and (100) surface of CdTe resulting from EAg and *N* etches.

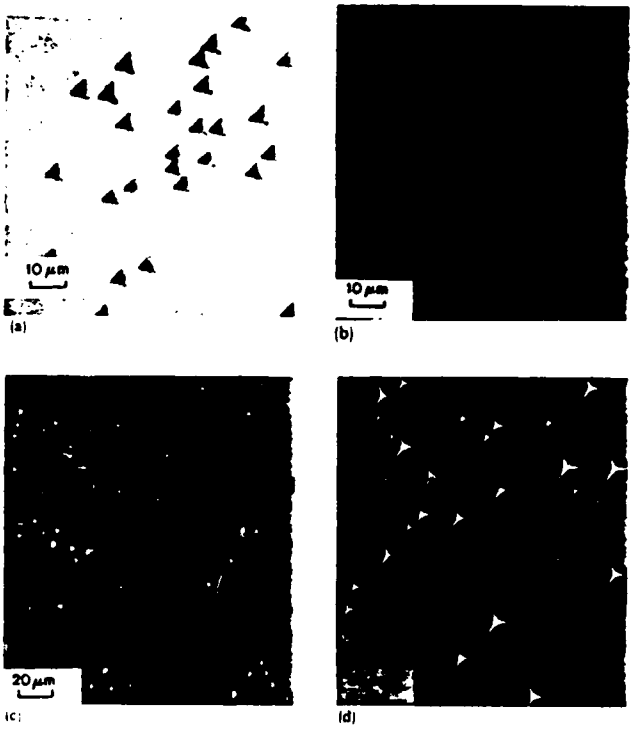

FIG. 2. (a) Aα pyramidal pits (E: 1 min; EAg 1: 1 min), (b) Bα flat bottomed pits (E: 1 min; EAg 1:1 min), (c) Aβ flat bottomed pits (E: 1.5 min; EAg 2:20 s, with stirring), (d) Bβ pyramidal pits (E: 1.5 min; EAG 2:20 s, with stirring).

EAg solutions with low Ag^+ concentrations under quiescent conditions produced well-formed etch figures of one type, as in Fig. 1. High Ag^+ solutions vigorously agitated, produced well defined etch figures of the opposite type. Intermediate conditions such as low Ag^+ vigorously agitated, or high Ag^+ under quiescent conditions produced etch figures of mixed character.

TABLE I. Chemical composition of polishing and etching solutions.

Symbol	Composition		Action
E (Ref. 1)	HNO_3	10 ml	
	H_2O	20 ml	polishing
	$K_2Cr_2O_7$	4 g	
EAg 1 (Ref. 1)	E solution	10 ml	
	$AgNO_3$	0.5 mg	etching
EAg 2 (Ref. 1)	E solution	10 ml	etching
	$AgNO_3$	10 mg	
N (Ref. 3)	H_2O	20 ml	etching
	H_2O_2	20 ml	
	HF	30 ml	

quiescent and agitated conditions. Agitation was by gas bubbler, teflon paddle, or by hand, and ranged from gentle to violent stirring. In parallel studies with the *N* solution, we first chemically polished with E solution for 1 min, then etched with the *N* solution for 20 to 60 s. This was immediately followed by a one-second dip in E solution to remove the dark stain that usually occurs when using *N* solution. All of the etching procedures were carried out at 23 °C, and in many cases both surfaces were etched at the same time to compare the size and morphology of the etch pits on opposite surfaces.

In certain instances, repeat etching or repeat polishing and etching were carried out to study the repeatability of the etching procedures. In these experiments the oriented samples remained on the nonreactive glass polishing fixture and only one side of each sample was etched. However, numerous samples were mounted on the fixture at one time, permitting the simultaneous study of both A and B surfaces. For the repeat polishing and etching experiments, the previous etching features were removed by chemomechanical polishing only. Total material removal in these cases was significantly less, on the order of 25 μm, which was determined by the known etching rates and the times required to eliminate the previous set of etch pits. Analysis of etch pit morphology and etch pit density was carried out using optical microscopy and scanning electron microscopy.

III. RESULTS

All orientations of CdTe surfaces, including randomly oriented grains on the edges of a number of samples, were found to form etch pits in EAg solutions. This was in contrast to the *N* solution which forms etch pits only on one CdTe(111) surface. The definition and morphology of the etch pit figures formed in EAg solutions was found to depend strongly on the Ag^+ concentration and agitation conditions. Those formed in *N* solutions were always shallow and roughly spherical in shape. In Fig. 1, a graphical representation is given of the etch pit morphologies observed, as a function of substrate orientation and etching conditions. Also shown are the relative size differences that were observed on etching both surfaces of the test samples at the same time. Noticeable size differences were, as expected, found only on the polar {111} surfaces. The graphical figures are somewhat idealized; in most cases the etch pits were not so perfectly formed. It was normally possible to determine from optical microscopy whether a set of characteristic etch pits was pyramidal or flat bottomed. However, SEM with its much greater depth of field and resolving power, was relied upon to provide additional details about the interior surfaces of the etch pits. Figure 2 shows photomicrographs of the four types of etch pits observed with EAg solutions, and Fig. 3 shows the type of etch pits typically seen with *N* solutions.

EAg solutions with low Ag^+ concentrations under quiescent conditions produced well-formed etch figures of one type, as in Fig. 1. High Ag^+ solutions vigorously agitated, produced well defined etch figures of the opposite type. Intermediate conditions such as low Ag^+ vigorously agitated, or high Ag^+ under quiescent conditions produced etch figures of mixed character.

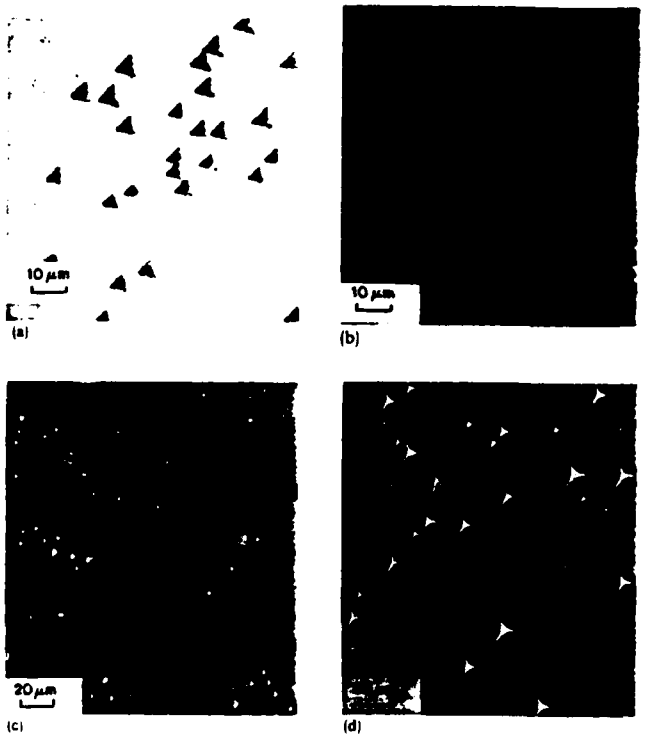

FIG. 2. (a) Aα pyramidal pits (E: 1 min; EAg 1: 1 min), (b) Bα flat bottomed pits (E: 1 min; EAg 1:1 min), (c) Aβ flat bottomed pits (E: 1.5 min; EAg 2:20 s, with stirring), (d) Bβ pyramidal pits (E: 1.5 min; EAG 2:20 s, with stirring).

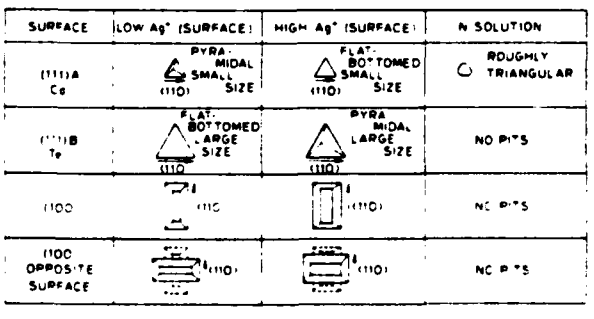

FIG. 1. Typical etch pit morphologies on (111) and (100) surface of CdTe resulting from EAg and *N* etches.

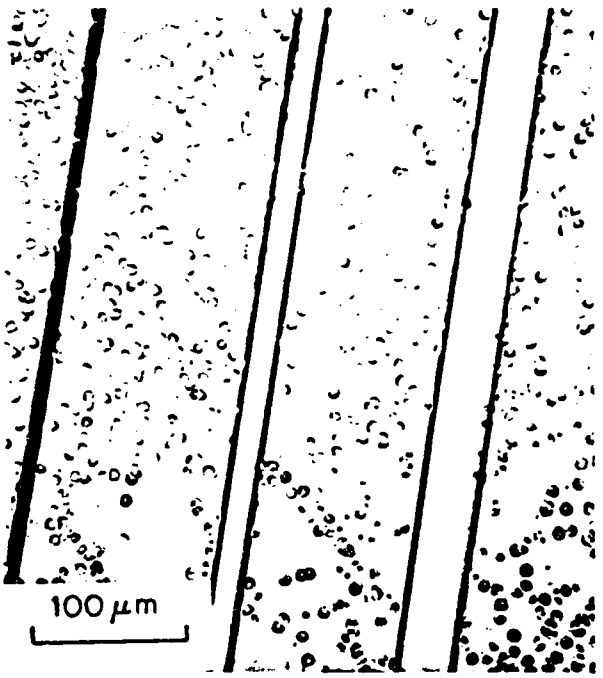

FIG. 3. Etch pits from N solution. The pits are roughly triangular, and there are no pits in the twinned region.

It was found with both EAg solutions, and N solution as well, that under repeated etching with no intermediate polishing steps, the etch pit patterns remained the same but the size of the etch pits became larger as the total accumulated etching time increased (see Fig. 4).

When EAg 1 (low Ag^+) etching was followed by EAg 2 (high Ag^+) our results were only partially consistent with the larger data base used to generate Fig. 1. On the (111)A surfaces no new etch pits were formed, but the etch pits existing after the first etch changed morphology from downward (pyramidal) pits to flat bottomed pits. On the (111)B surfaces initially flat bottomed pits remained flat bottomed, but new pits which formed as a result of the second etch did have the expected downward character. Where EAg 2 was followed by EAg 1, the (111)A surface behaved as in the previous case: no new pits were formed, but their character changed from flat bottomed to downward pits. On the (111)B surfaces, most of the pits observed tended toward a flat bottomed character, but the total number increased significantly as a result of the second etch in EAg 1.

Numerous experiments were carried out in repeat polish and etch sequences to determine whether characteristic arrays of etch pits would repeat, or if it was possible to follow individual dislocations. In no case, however, were we able to produce similar etch pit patterns whenever there was an intermediate chemomechanical polishing step no matter what the combination of etching solutions used. Etch pit densities revealed by each of the etching solutions tended to be consistent during repeat polish and etch sequences to well within an order of magnitude. The relative pit densities revealed by the different etches on the same surface varied considerably, however, in the order $N >$ EAg 1 $>$ EAg 2 where the symbol denotes the relative etch pit density revealed with that etch.

Several {111} substrates were polished to thicknesses of 500 μm or less, and the etch pit patterns which were generated by simultaneously etching both surfaces in either EAg 1

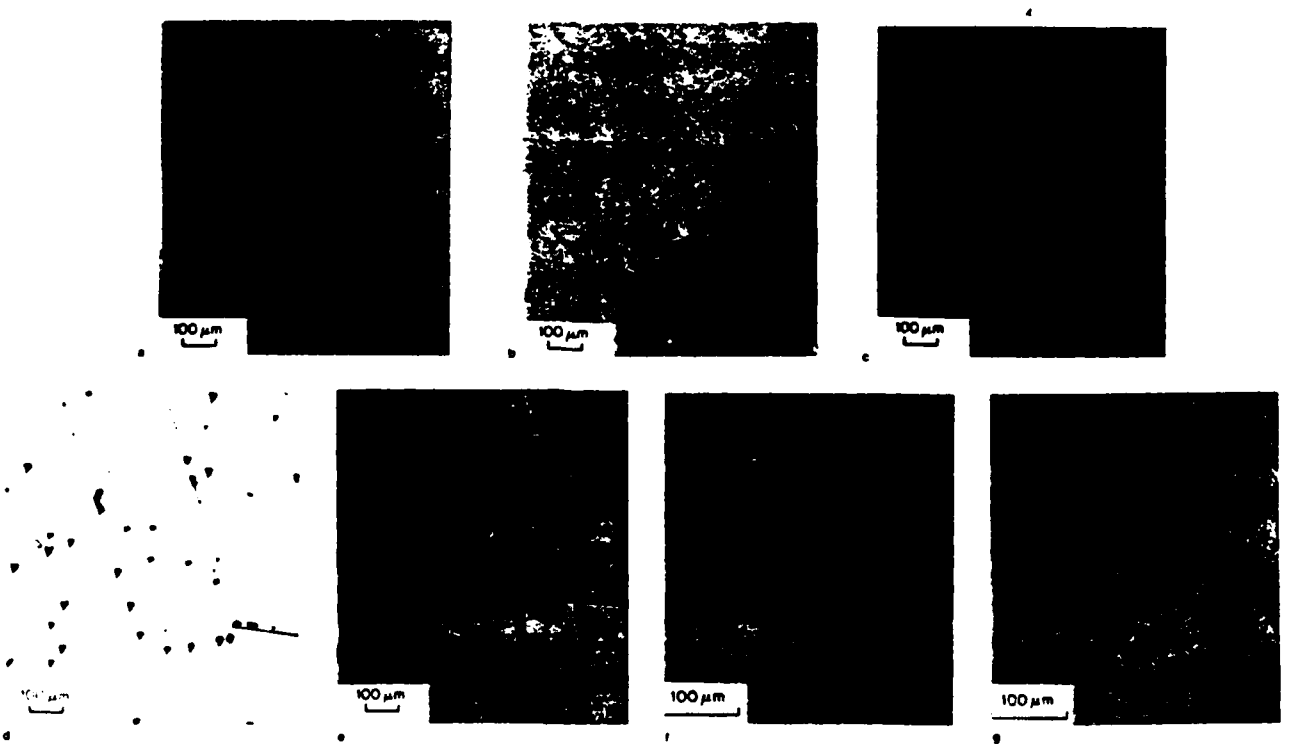

FIG. 4. Time development of etch pits: (a)–(c) using EAg 1, and E: 30 s, (a) 20 s, (b) 40 s, (c) 60 s, (d) and (e) using EAg2, same area, and E: 1 min, (d) 30 s, (e) 60 s. (f) and (g) using N, and E: 1 min, (f) 20 s, and (g) 40 s.

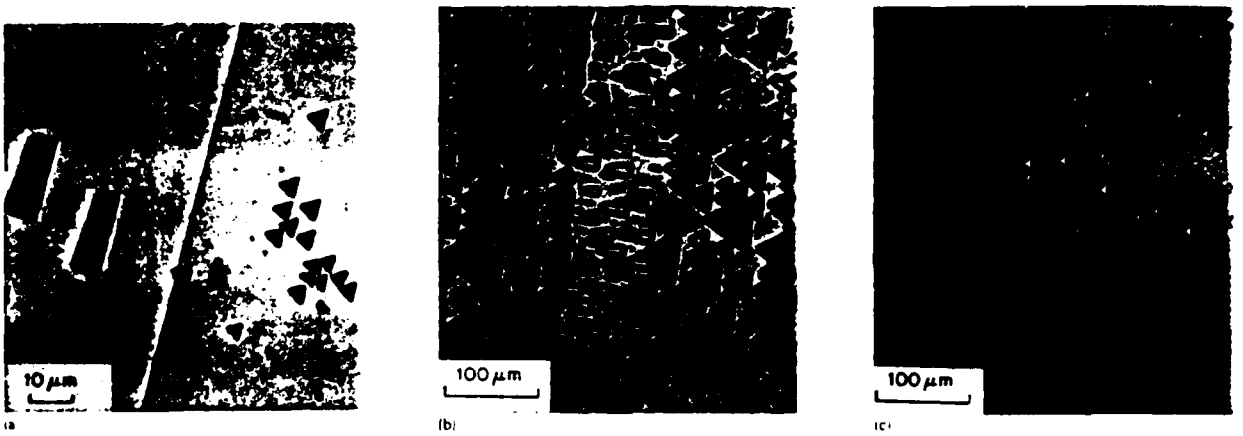

FIG. 5. (a) Etch pits near twin boundary (E 1.5 min; EAg 1:1 min). At low Ag^+ concentration, the long sides of the rectangular pits are parallel to the twin boundary when the neighboring pits are pyramidal (Aα). The twinned region is 16.8° off the (100). (b) Twinned region of surface opposite to that shown in (a) (E: 1.5 min, EAg2: 1 min, no stirring) showing the low Ag^+ characteristic. The long sides of the rectangular pits are perpendicular to the twin boundary when the neighboring pits are flat bottomed (Bα). There are also a few pyramidal pits. (c) Same surface as in (b), EAg 2 etch, 20 s, with vigorous stirring. The triangular pits become pyramidal, with no 60° rotation; the aspect ratio of the rectangular pits decreases.

or EAg 2 were observed by IR transmission microscopy. No obvious one-to-one correlation could be made by comparing top and bottom surface etch pit patterns. Similar experiments were also carried out, etching the top surface with EAg 1 and the bottom surface with EAg 2, sequentially, and then comparing etch pit patterns. Again, no obvious one-to-one correlation could be made.

The *N* solution was observed to produce etch pits only on the surface which formed pyramidal pits when etched by EAg 1.

Finally, scanning electron microprobe analysis seemed to indicate that there was a relatively uniform chemisorbed layer of Ag^+ ions on both the (111)A and (111)B surfaces. Little data could be obtained from the interiors of the pyramidal etch pits, however, because of geometrical shadowing effects.

IV. DISCUSSION

Our results were in basic agreement with the work reported by Inoue, but some differences were noted. A new finding was the appearance of small flat bottomed pits on {111}A planes when etched with EAg 2, (Fig. 2). According to Inoue, high Ag^+ etches reveal tellurium (β) edge dislocations.

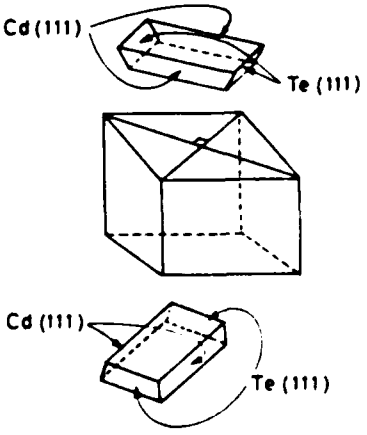

FIG. 6. Orientation of (100) etch pits on opposite surfaces, showing 90° rotation.

The appearance of this type of etch pit may be the first time that Aβ dislocation pits have been seen in CdTe.

Characteristically different types of etch pits were observed on (111)B surfaces using EAg 1 and EAg 2. However, in our case, their geometric orientation remained the same, while in the work of Inoue, a 60° rotation about the surface normal was reported. In Fig. 5, we show optical micrographs of two samples cut sequentially, each of which contained several lamellar twins. One was etched in EAg 1 and the other in EAg 2. In the (111) regions where triangular etch pits are seen, well-formed etch figures are apparent but a 60° rotation is not seen. Nor was a 60° rotation observed in the repeat etch experiments where only a single substrate was used. This result is not consistent with the argument by Inoue that the etch pits formed by EAg solutions are interior tetrahedral voids bounded by the slowest etching planes which should be either the (111)A or the (111)B depending on the etching solution used. The Inoue model is consistent with the concept of chemical attack on slow etching {111} planes occurring primarily at kink sites in a layer-by-layer fashion. It predicts a 60° rotation in etch pit orientation if the slowest etching {111} planes are actually reversed from A to B with an increase in Ag^+ concentration in the etching solution. Our initial conclusion is that we were not able in our experiments to reverse the slow etching {111} planes by simply increasing the Ag^+ concentration.

Additional evidence for this conclusion is obtained from our results on (100) substrate orientations. In the zinc-blende structure the ⟨100⟩ axes have fourfold inversion ($\bar{4}$) symmetry, and such symmetry should cause a 90° rotation of the etch pits on opposite surfaces, as shown graphically in Figs. 1 and 6. The (100) pits are bounded by two pairs of opposite (111) planes, one pair being Cd(111) planes, the other pair Te(111) planes. The dissolution rate of Te is higher than that of Cd in low Ag^+ concentration etching solutions, so we expect the long sides of the rectangular pits to be the Cd surfaces and the shorter sides the Te(111) surfaces.

On the opposite side of the substrate, the polarity of the (111) planes bounding the pits is reversed, and therefore, the

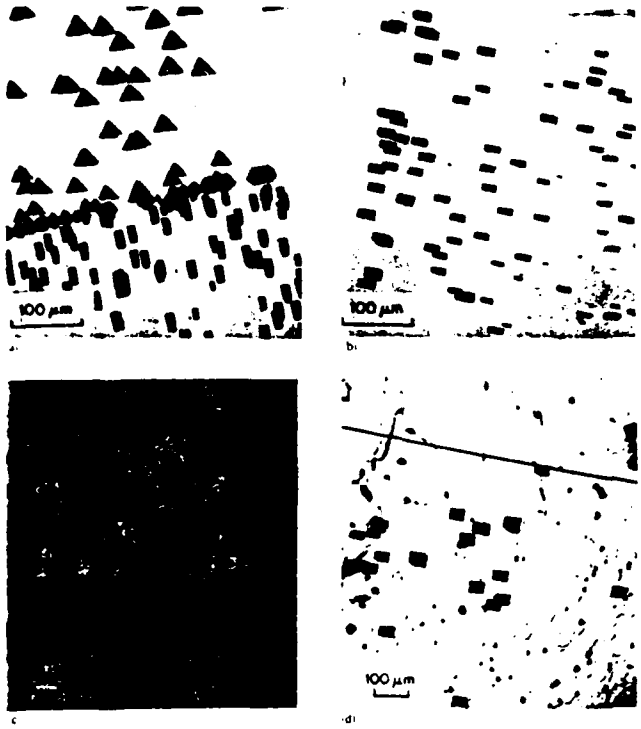

FIG. 7. Etch pit morphology change on (100) surfaces. (a) and (b) show opposite surfaces, etched by EAg 1 (20 s), (c) and (d) are the same pair of surfaces, etched by EAg 2 (20 s, with stirring). The surfaces are intersected by twin boundaries.

rectangular pits should rotate 90°, consistent with the $\bar{4}$ symmetry. This rotation was observed in EAg 1 solutions, and is shown in Figs. 7(a) and 7(b).

For high Ag^+ concentrations, the chemical reactivity of Cd and Te was expected to be reversed and the rectangular pits on a (100) substrate were expected to rotate 90° as the Ag^+ concentration was changed from low to high levels. The rectangular pits were not observed to rotate. However, the ratio of width to length increased, and some pits were square [see Figs. 7(c) and 7(d)].

In our etching studies we found that agitation had the same effect as increasing the Ag^+ concentration. Etching of InSb by modified CP4 solutions has been shown to be diffusion controlled at 23 °C.[7] The temperature dependence of the chemical dissolution rates was not measured in this study, but the results of agitation strongly suggest that etching in the CdTe/EAg system is also diffusion controlled.

A one-to-one correspondence of etch pits on opposite surfaces was not observed except for those pits at the corners of the twin boundaries. A possible explanation for this is that the pits may not all be revealed, or the inclination and wandering of dislocations may make it difficult to trace the dislocation path. Those pits revealed on the twin boundaries are probably twin pits, as Kumagawa showed.[8]

It was found that the *N* solution pits those surfaces which formed pyramidal pits on etching by EAg 1. Nakagawa[3] identified this surface as the (111)B, probably using the x-ray results by Warekois.[6] However, Inoue *et al.*[1,2] identified it as the (111)A surface. Recently, Fewster *et al.*[9] used anomalous x-ray absorption on (Hg, Cd)Te and found that the (111)A is

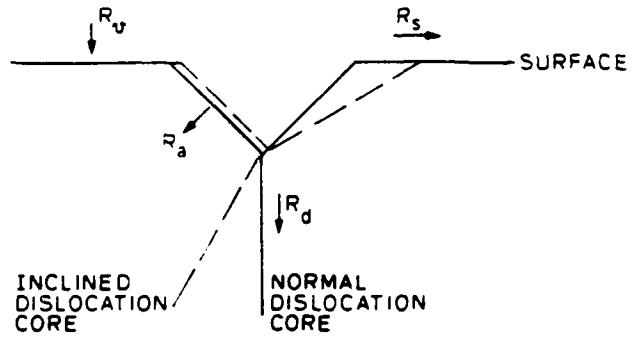

FIG. 8. Etching rates which determine the etch pit morphology.

the surface which was pitted. The same result was also found for CdTe.[10] Our results confirm that the Nakagawa etch pits the (111)A surface of CdTe.

V. PREFERENTIAL ETCHING AT DISLOCATIONS

Preferential etching at dislocation sites is a very complex phenomenon that is not fully understood.[11] Referring to Fig. 8, the formation of etch pits along dislocation lines depends on the relative magnitude of several of the following dissolution rates:

R_s = dissolution rate along surface;

R_a = dissolution rate normal to the planes at an angle to surfaces;

R_v = dissolution rate normal to surface;

R_d = dissolution rate along dislocation.

If the etching rate along the dislocation is much greater than that normal to the surface ($R_d \gg R_v$) the pits will be deep. Otherwise they will be shallow or may not even form. If the etching rate R_a is large, the pits will be large. If the dislocation cores are inclined to the surface, the shape of the etch pit will be distorted as indicated by the broken lines. Additional factors such as kink site removal and the energetics of slow etching planes are required to account for well-defined etch figures.

The species $(Cr_2O_7)^{-2}$ and $(NO_3)^-$ in the EAg solutions are strong oxidizers and are likely to react vigorously with surface Te atoms. They are also expected to rapidly attack and simply dissolve away any Cd surface atoms. In his original work, Inoue[1] proposed that Ag^+ ions might substitute for exposed Cd atoms, and this would account for the etch rate reductions he observed on (111)A surfaces with Ag^+ addition. The reported reduction in dissolution rates on (111)B surfaces with increasing Ag^+ concentration seems harder to explain by Ag replacement of Cd. An alternative model in the case of (111)B surfaces is the adsorption poisoning model which was used to predict the etching behavior of InSb in oxidizing etches by Gatos *et al.*[12–14] Theirs is a modification of the model of preferential etching at dislocation sites due to Cabrera.[15] If we assume that the (111)B surfaces are strongly electronegative in character due to the high ionicity of CdTe (0.717 on the Philips scale[16]) significant adsorp-

tion poisoning by Ag^+ ions seems likely. Also, strong chemical reactivity is implied and this agrees with the high dissolution rates observed on (111)B planes. In this work, we propose that Ag^+ acts only as a poisoner on exposed Te sites and is the chemical reaction rate determining factor on both (111)A and (111)B surfaces.

To determine under which conditions the two types of edge dislocation cores Cd(α) or Te(β) might produce etch pits when Ag^+ ions are present in the etching solution, it is necessary to evaluate qualitatively the relative reaction rates referred to in Fig. 8. Not much is known about the precise chemical reactions that go on in this system, and consequently it is only possible to estimate relative reaction rates. We consider only the polar {111} surfaces and separate the low and high Ag^+ cases in the same format used by Gatos *et al.*[12–14] Arguments paralleling theirs are proposed for each of the four combinations Aα, Aβ, Bα, and Bβ, first in the low Ag^+ case and then in the idealized high Ag^+ case.

A. Low Ag^+ (EAg 1) solution

In low Ag^+ etching solutions, we assume that the dissolution rate of the {111}B surface is significantly faster than that of the {111}A surface, even though it is the B surface that is selectively adsorption poisoned.

1. Aα case (Cd dislocation intersecting a {111}A surface)

The terminal atom of a Cd dislocation is located in the surface plane of atoms. Therefore, it is doubly bonded (A2) and consequently more reactive than a triply bonded A surface atom (A3). (This notation follows that of Gatos.[11]) Removal of the A2 atom exposes two triply bonded B atoms (B3), but the B3 are more reactive than the A3 surface atoms and will be removed easily; therefore, four A3 surface atoms are exposed as well as the next A2 dislocation terminal atom. Because the newly exposed A2 atoms are always more reactive than the three adjacent A3 atoms, the etching proceeds more rapidly along the dislocation than on the surface, resulting in the formation of dislocation etch pits with pointed pyramidal characteristics.

2. Aβ case (Te dislocation intersecting a {111}A surface)

The terminal Te dislocation B atom is not in the outermost layer of the surface and so it is difficult to initiate an etch pit. Even if this B3 atom reacts faster and is removed faster than the surface A3 atom, the two exposed A2 atoms on the surface are probably more reactive than the next dislocation terminal atom bonded by three A3 atoms. Thus there is minimal preferential attack along the dislocation line.

3. Bα case (Cd dislocation intersecting a {111}B surface)

In III–V compounds, the difference in chemical reactivity between the A and B atoms is small. Consequently only Aα pits are formed.[12–14] However, because of the higher ionicity in CdTe and the higher reactivity of Te surface atoms, the Te atomic layer is much more easily removed than the Cd layer.

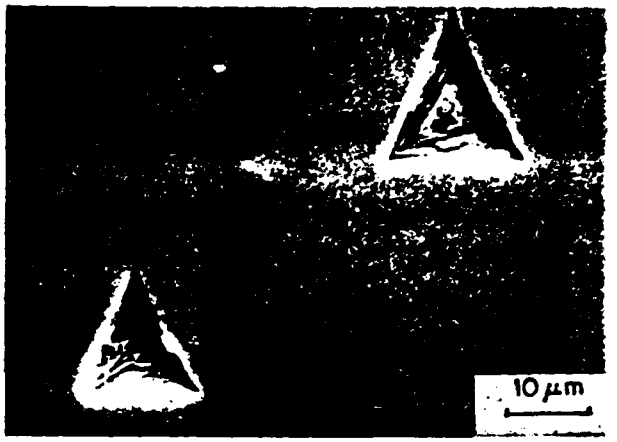

FIG. 9. Scanning electron micrograph showing pyramidal and flat bottomed pits on the same surface (E: 1 min, and EAg2:25 s, gentle stirring).

Although the removal of a single Te surface layer is highly unlikely, because of the nature of the bonding with the adjacent Cd layer, we can imagine a transient state in which the dislocations effectively behave as if they had Aα character. Such a transient state might then favor the formation of Bα pits. A higher etching rate in the neighboring region relative to the true Aα case could account for the fact that Bα pits are flatbottomed, while the Aα are pyramidal.

4. Bβ dislocations (Te dislocation intersecting a {111} B surface)

Bβ pits are not observed in InSb.[12] Even assuming a transient B$\beta \rightarrow$Aβ condition, Bβ pits are not expected since Aβ dislocations do not readily produce etch pits.

B. High Ag^+ (EAg2) solution

In the ideal case, as the Ag^+ ion concentration increases, the relative chemical reactivity of Cd and Te should eventually be reversed as the exposed Te atoms are poisoned. Thus the favorable conditions for etch pit formation would be reversed, and in high effective Ag^+ concentrations, we might expect Aβ and Bβ pits instead of Aα and Bα. The Aβ pits should be triangular with flat bottoms and the Bβ pits should be pyramidal.

Frank,[17] in a work in the kinematic theory of dissolution processes, pointed out that poisoner depletion can occur if the adsorbed species is removed as a complex which must first decompose before it can be readsorbed again. Since the B surfaces etch faster and produce larger pits even in high Ag^+ solutions, this may be evidence of Ag^+ depletion. We therefore postulate that local Ag^+ depletion may be part of the reason why we did not observe etching rate reversal in these experiments. In our model, the etching process is thought to be diffusion controlled, with the local effective Ag^+ concentration playing the key role. Agitation clearly increases the effective Ag^+ concentration, but Ag^+ ion depletion could decrease it in local regions. This effect might inhibit reversal of chemical etching rates and explain why mixed features (pyramidal and flat bottomed pits) were seen on the same surface (Fig. 9) and why 60° rotation of etch pits was not seen on (111) substrates nor 90° rotation on (100) substrates.

VI. CONCLUSIONS

EAg solutions reveal more types of dislocations than the Nakagawa etch and they can be used for determination of the polarity of {111} surfaces. Aβ dislocations were revealed for the first time in CdTe.

In spite of great care to remove polishing damage and to achieve a reproducible etching technique, the EAg etches consistently gave lower etch pit densities than those obtained with the Nakagawa etch. The EAg solutions did give etch pit densities consistent to within an order of magnitude, and thus can be used to compare the relative quality of different samples. However, neither the Inoue nor the Nakagawa etch pit densities has yet been correlated with dislocation density on a one-to-one basis.

The observed etch pit morphologies were explained using an adsorption poisoning theory originally proposed for III–V semiconductors by Gatos and Lavine. This extension of the theory gives a good explanation of the observed phenomena provided that allowance is made for the higher ionicity of CdTe. Stirring changes the etch pit morphology, suggesting diffusion control at room temperature. Interface control may be possible at lower temperatures.

Complete reversal of chemical reactivity on increasing the Ag^+ ion concentration in EAg etches was not achieved. For example, 60° rotation of etch pits on the (111) surfaces was not observed, nor was 90° rotation on the (100) surface observed.

It was confirmed that the Nakagawa solution produced etch pits only in the (111)Cd surfaces.

Our understanding of preferential etching is still qualitative and more knowledge of the detailed surface chemical reactions and surface reconstruction is needed. An etch which can give quantitative dislocation densities in CdTe is still lacking.

ACKNOWLEDGMENTS

This work was supported by the U.S. Army Research Office Contract No. DAAG29-83-K-0023 and the NSF–MRL Program through the Center for Materials Research at Stanford University.

[1]M. Inoue, I. Teramoto, and S. Takayanagi, J. Appl. Phys. **33**, 2578 (1962).
[2]M. Inoue, I. Teramoto, and S. Takayanagi, J. Appl. Phys. **34**, 404 (1963).
[3]K. Nakagawa, K. Maeda, and S. Takeuchi, Appl. Phys. Lett. **34**, 574 (1979).
[4]A. K. Chin, J. Electrochem. Soc. **129**, 369 (1982).
[5]H. Iwanaga and T. Yoshiie, J. Cryst. Growth **61**, 691 (1983).
[6]E. P. Warekois, M. C. Lavine, A. N. Mariano, and H. C. Gatos, J. Appl Phys. **33**, 690 (1962).
[7]H. C. Gatos and M. C. Lavine, J. Phys. Chem. Solids **14**, 169 (1960).
[8]M. Kumagawa, Jpn. J. Appl. Phys. **21**, 804 (1982).
[9]P. F. Fewster, S. Cole, A. F. W. Willoughby, and M. Brown, J. Appl. Phys **52**, 4568 (1981).
[10]P. F. Fewster and P. A. C. Whiffin, J. Appl. Phys. **54**, 4668 (1983).
[11]H. C. Gatos, *Crystal Growth and Characterization*, edited by R. Ueda and J. B. Mullin (North Holland, Amsterdam, 1975), p. 311.
[12]H. C. Gatos and M. C. Lavine, J. Electrochem. Soc. **107**, 427 (1960).
[13]H. C. Gatos and M. C. Lavine, J. Electrochem. Soc. **107**, 433 (1960).
[14]M. C. Lavine, H. C. Gatos, and M. C. Finn, J. Electrochem. Soc. **108**, 974 (1961).
[15]N. Cabrera, J. Chem. Phys. **23**, 675 (1956).
[16]J. C. Phillips, *Bonds and Bands in Semiconductors* (Academic, New York, 1973), p. 42.
[17]F. C. Frank, *Growth and Perfection of Crystals*, edited by R. Doremus, B Roberts, and D. Turnbull (Wiley, New York, 1958), p. 411.

END

FILMED

9-85

DTIC